NTNU
Norwegian University of
Science and Technology

Numerical Modeling and Analysis of a Semi-submersible Fish-cage

Rui Dou

Numerical Modeling and Analysis of a Semi-submersible Fish-cage

Rui Dou

MASTER THESIS

Department of Marine Technology

Norwegian University of Science and Technology

June 2018

Trondheim, Norway

NTNU Trondheim
Norwegian University of Science and Technology
Department of Marine Technology – Group of Marine Structures

MSC THESIS IN MARINE TECHNOLOGY
SPRING 2018
FOR

Rui Dou

Numerical Modelling for Dynamic Response Analysis of a Rigid Fish Cage Structure in Regular Waves

Background:
Due to the increasing demand for salmon internationally and the fast development of the aquaculture industry in Norway, fish farms are moving from well-protected fjords to more open seas. This requires new design of fish farms. The Norwegian company SalMar has developed and is now operating a more rigid semi-submersible-type floating fish cage, Ocean Farm 1. It is a circular floater with 12 columns connected by braces, which formulates a relatively rigid frame for attaching nets. It is moored by in total 8 catenary mooring lines at 4 columns. The complexity in hydrodynamic loads on the floater and the nets as well as the coupling between the motions of the floater and the mooring system make it difficult to estimate properly the motion and structural responses of the complete system.

The purpose of this thesis is to establish a time-domain model in SIMA for dynamic response analysis of the Ocean Farm 1 structure and to study the dynamic performance of the system in waves. In particular, the focus should be given to the modelling of the wave loads on the nets and the contribution to the total wave loads on the floater using the External Force DLL in SIMA.

This thesis topic is proposed by Sintef Ocean and the thesis work will be co-supervised by Dr. Biao Su at Sintef Ocean. The overall dimensions of the Ocean Farm 1 concept will be given to the student.

Assignment:
The following tasks should be addressed in the thesis work:
1. Carry out a literature review on modelling and analysis of aquaculture plants, with focus on wave loads on net panels and dynamic response analysis of moored floating structures.

2. Establish a hydrodynamic model (including a panel model, a Morison drag model and an FE-based mass model) of the Ocean Farm 1 floater (excluding the nets) in HydroD and perform a hydrodynamic analysis to obtain the hydrodynamic loads coefficients.

3. Study how to use the software SIMA. Based on the hydrodynamic data from the HydroD analysis, establish a time-domain model of the floater and its mooring system. The Morison drag model should be again established in SIMA.

4. Establish the wave loads model on nets using the screen model approach. Properly consider the water particle velocity and the floater motion-induced velocity of each net panel as well as the angle between the relative velocity and the normal direction of each panel. Make a Fortran code to calculate the total forces and moments due to the distributed loads on net panels of the floater, and use it as External Force DLL for time-domain simulations in SIMA.

5. Validate the developed DLL for the case of current only, against the published data. Perform regular wave analysis considering different combinations of wave height and periods. Discuss and compare the obtained first-order wave loads on the floater, the drag loads on the nets and their induced motions of the floater and mooring line tension.

6. Conclude the work and give recommendations for future work.

7. Write the MSc thesis report.

In the thesis the candidate shall present his personal contribution to the resolution of problem within the scope of the thesis work.

Theories and conclusions should be based on mathematical derivations and/or logic reasoning identifying the various steps in the deduction.

The candidate should utilize the existing possibilities for obtaining relevant literature.

The thesis should be organized in a rational manner to give a clear exposition of results, assessments, and conclusions. The text should be brief and to the point, with a clear language. Telegraphic language should be avoided.

The thesis shall contain the following elements: A text defining the scope, preface, list of contents, summary, main body of thesis, conclusions with recommendations for further work, list of symbols and acronyms, reference and (optional) appendices. All figures, tables and equations shall be numerated.

The supervisor may require that the candidate, in an early stage of the work, present a written plan for the completion of the work. The plan should include a budget for the use of computer and laboratory resources that will be charged to the department. Overruns shall be reported to the supervisor.

The original contribution of the candidate and material taken from other sources shall be clearly defined. Work from other sources shall be properly referenced using an acknowledged referencing system.

The thesis shall be submitted electronically (pdf) in DAIM:
- Signed by the candidate
- The text defining the scope (this text) (signed by the supervisor) included
- Computer code, input files, videos and other electronic appendages can be uploaded in a zip-file in DAIM. Any electronic appendages shall be listed in the main thesis.

The candidate will receive a printed copy of the thesis.

Supervisor: NTNU: Prof. Zhen Gao
Co-supervisor: Sintef Ocean: Dr. Biao Su; KTH: Assoc. Prof. Zuheir Barsoum
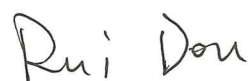
Deadline for thesis report: 11.06.2018

Preface

This thesis work is part of my double degree master study at Marine Technology Department in NTNU and Department of Aeronautical and Vehicle Engineering in KTH. It is also a collaborative research with SINTEF OCEAN. I started with literature review and theory studies during the autumn semester in 2017. Modeling and calculation were carried out in spring and summer in 2018.

The research object is a semi-submersible fish cage Ocean Farm 1. It arrived at Frohavet in August 2017 and it's exciting to study on the world's first offshore fish farm. The work has been challenging, especially when modeling a huge structure and combining time domain analysis with external programming. It was stressful and frustrating in the last month with a divergent result. I felt so lucky when finally the reason of errors was found and good result came. I hope this thesis study can make some contribution to aquaculture and there will be a boom production of salmon as well as lower price.

I have gained a lot during the thesis. not only a deeper understanding on theories, but also always to stay calm and structured.

Trondheim, June 9, 2018

Rui Dou

Acknowledgment

Summary

The concept of rigid fish-farm was raised to overcome the space limitation of traditional fish-farm. To ensure that the structure has the ability to withstand the harsh sea environment, this report investigates a rigid semi-submersible fish-farm.

The study object is Ocean Farm 1. FEM model of Ocean Farm 1 has been built in GeniE. Considering the dimension difference of structure components, larger parts, like pontoons and main columns were built with panel elements, while slender beams were modeled by Morison elements. A mass model has been built to provide a more precise mass distribution and correct position of center of gravity. Total number of elements of FEM model was up to 14380. Hydrodynamic calculations were accomplished in HydroD with all FEM model input. Mass matrix, damping matrix and RAOs were calculated in frequency, range from 0-2 rad/s.

Hydrodynamic results were saved in G1 file and input to SIMA for time domain response calculation. Morison elements in previous FEM model were rebuilt as slender elements to take drag force into consideration. Furthermore, wave force on net was also included, which was carried out by an external communicative file. Environment condition was determined by sea states in Frohavet sea. Current velocity was taken as 0.75 m/s and results were verified with previous research. Twelve wave states wre also studied. Comparisons were made between model with and without net force, as well as responses under different wave condition.

Contents

x

List of Figures

List of Tables

Nomenclature

Acronyms

DOF Degree of freedom

FAO Food and Agriculture Organization

FEM Finite element method

FRC Floating rigid cage

MSI Marina System Iberica

RAO Response amplitude operator

$SIMA$ Simulation Workbench for Marine Applications

SRC Submersible rigid cage

$SSFC$ Semi-submersible flexible cage

VCG Vertical center of gravity

Roman Letters

η Body motion

γ Transformation matrix

λ Wave length

ν Poisson's ratio

ω Wave frequency

ϕ Wave potential / Rotation angle around the global x-axis

ψ Rotation angle around the global z-axis

ρ Density of the material/fluid

ρ' Average density

σ_y Yield strength of the material

θ Angle between relation motion and panel normal vector   Rotation angle around the global y-axis

ζ	Wave elevation
ζ_0	Wave amplitude
$Y(\omega)$	Transfer function

Greek Symbols

A	Area of the cross-section / Width of a net mesh
B	Pitch of a net mesh
C	Height of a net mesh
C_A	Added mass coefficient
C_d	Drag coefficient
C_l	Lift coefficient
$C_{d,screen}$	Drag coefficient of screen panel
$C_{l,screen}$	Lift coefficient of screen panel
D	Diagonal length of a net mesh / Diameter of a cylinder
E	Young's modulus
F_d	Drag force
F_l	Lift force
f_N	Sectional wave force of Morison elements
g	Gravity acceleration
h	Water depth
H_S	Significant wave height of irregular wave
k	Wave number
Sn_{model}	Solidity ratio of the panel model
T	Wire thickness of the net / Regular wave period
T_Z	Zero-crossing period of irregular wave
u	Wave velocity in x direction
u_n	Velocity in the normal direction of a cylinder
$U_{C,100}$	100-year current velocity
w	Wave velocity in z direction
x^G	Vector in global coordinate system
x^L	Vector in local coordinate system

Chapter 1

Introduction

1.1   Background

Aquaculture plays a more and more important role in fishing industry. By statistics from FAO(Food and Agriculture Organization)[1], Norway produced 3.5 million tonnes of seafood in 2009, in which about 25 percent were coming from the aquaculture industry. And it has been increasing as shown in figure 1.1[2]. In the past decades, fish farming has moved to open sites . The trend of larger farms in exposed areas has inspired new fish farm concepts [15].
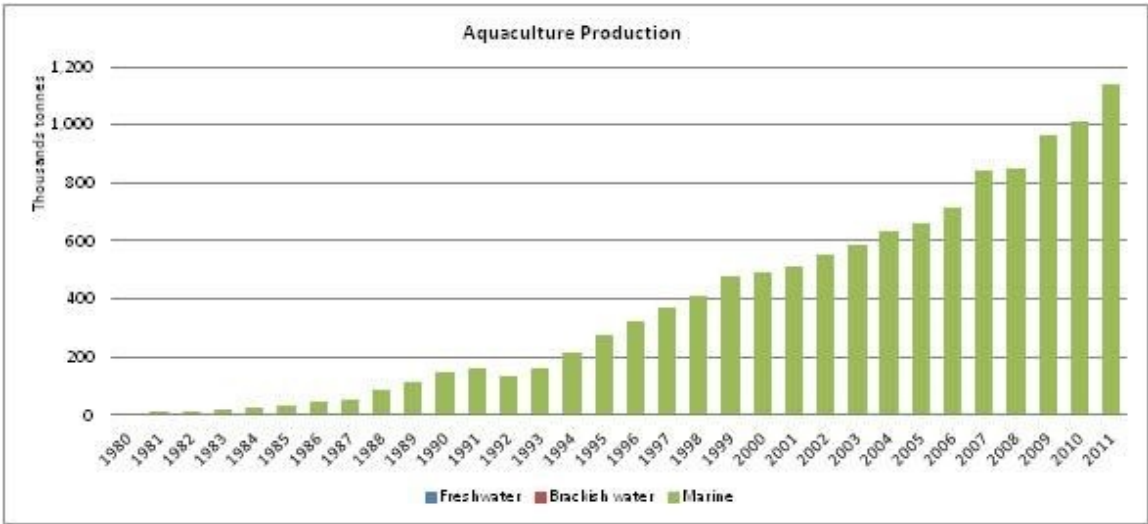
Figure 1.1: Aquaculture production in Norway

- Floating rigid cage (FRC)

Pisbarca(figure 1.2(a)) built by MSI(Marina System Iberica) is a hexagonal structure [3]. Instead of moving with wave and current, it is designed to withstand the environment loads. A obvious advantage is the stability for operations. But the large and heavy structure increase the difficulty to transportation and installation.

- Submersible rigid cage (SRC)

Submersible cage can avoid the water surface effect at the sea, and also would not cause any trouble for passing vessels. SADCO proposed a submersible concept [4] as shown in figure 1.2(b). Besides the small environment effect, the lack of visibility can also be a disadvantage for monitoring.

- Semi-submersible flexible cage (SSFC)

Refa cage with with tension leg in figure 1.2(c) can hold a relative stable volume[5]. But the harvest accessibility is limited and building cost is higher compared with other farm concepts.

(a) Pisbarca, FRC [14]   (b) SADCO, SRC [4]   (c) Refa, SSFC [5]
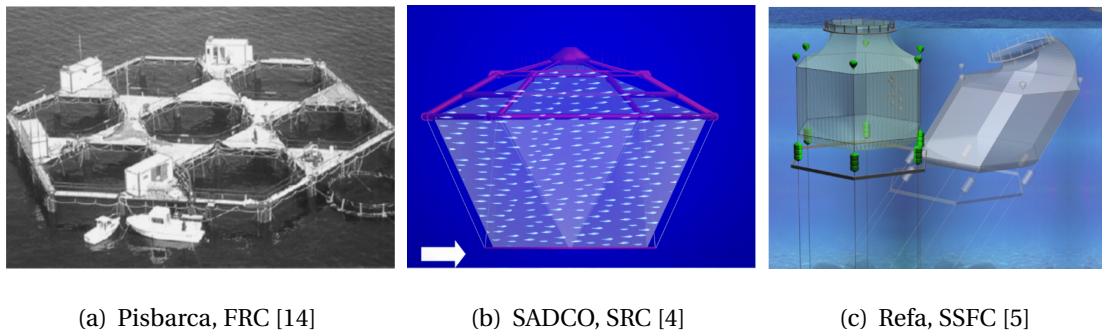
Figure 1.2: Different cage concepts

- Semi-submersible rigid cage

Ocean Farm 1, designed by Global Maritime, is a newly installed semi-submersible rigid cage(figure 1.1). It is suitble for water depth of 100 to 300 meters with a full-scale pilot facility. It is mainly composed of floating pontoons, slender frames and mooring system[6].

In this report, the research addresses response analysis of a rigid semi-submersible fish farm and Ocean Farm 1 is taken as the modeling object.

Figure 1.3: Over view of Ocean Farm 1 concept [7]

1.2 Problem Definition

1.2.1 FEM Modeling

A proper FEM model is the basis of all the further process. The FEM model built in this thesis includes three separate parts.

A panel model representing pontoons and columns should be built as the main structure. It is a great challenge to model a huge structure as correctly as possible when there is a limit of maximum finite element number. Therefore, some parts of structure are model with relative coarse elements and different mesh methods should be applied.

For slender beams, viscous effect should be considered and a Morison model for slender elements is needed to take drag force into consideration.

Mass distribution matters when deciding gravity center and mass matrix. Besides the mass of steel structure modeled by finite elements, mass of upper structure and other weighted elements should also be included in mass calculation. A separate mass model is built to meet the designed total weight and correct gravity center position.

3

1.2.2 Net Force Calculation

The net area on the cage is about 20000 m^2. Therefore, wave force on the net cannot be neglected. However, it's not practical to model all the net elements as large fishing cage contains millions of net elements. In this thesis study, screen model has been applied for net force calculation, in which the wave force is related to hydrodynamic coefficients. Those coefficients are determined by attack angle and relative motion of the structure, which means they are varying instantaneously and not a constant.

In SIMA software, such instantaneous force calculation cannot be realized. The proposed solution in this thesis is to create an external communicative file to complete the net force calculation.

1.3 Outline of the Thesis

The thesis is organized as follows:

In chapter 1, a brief introduction of Norwegian aquaculture background is summarized and different fish cage concepts are compared. Main researching problems in the thesis are presented.

In chapter 2, a thorough literature review of previous researches on aquaculture structure and net force calculation are listed.

In chapter 3, the modeling object, ocean Farm 1 is introduced. Parameters regarding the main structure, mooring system and cage net are presented.

In chapter 4, the applied theories in this thesis are explained, which including wave theory, sea loads analysis, motion calculation and screen model regarding net force calculation. DNV rules are also briefly summarized for some applied experience formula. Some preliminary calculations are made and results to be used in further modeling have been listed.

In chapter 5, the complete modeling and calculation process are explained step by step. FEM model in GeniE are discussed in detail. Hydrodynamic calculation settings in HydroD are summarized. Matrix and RAO results in frequency domain are covered. Modeling and analysis in SIMA are introduced and programming approach regarding external file is explained.

In chapter 6, results of calculations under different sea states are presented and categorize into several groups for better comparison and analysis. Conclusions are also summarized in this chapter.

In chapter 7, a summary of this thesis is made and intended future works are recommended.

Appendix gives some information on the software applied for the calculation.

Chapter 2

Literature Review

Literature regarding rigid-structured semi-submersible fish cage are in a limited searching field. Researches on other types of fish cage but bringing up motivating ideas for this thesis are also included here. The contents listed in this chapter are divided into two parts: structure study and net force calculation methods.

2.1 Previous Studies on Aquaculture Structure

2.1.1 Rigid Semi-submersible Cage

Li and Ong [17] did a preliminary hydrodynamic and response analysis on semi-submersible fish farm. Added mass and potential damping were calculated by linear potential theory. RAO was solved in frequency domain. The model they studied was treated as a large volume structure. 5 model methods were selected and results were compared.

- Pure panel model, no viscous damping;

- Panel model with viscous damping on braces;

- Panel model with viscous damping on braces and lower pontoons;

- Panel model with viscous damping on braces and both upper and lower pontoons;

- Pure Morison model with equivalent coefficients;

- Panel model with viscous damping and simplified net cage elements.

7

It shows that Morison model was not applicable as the the structure was semi-submersible while Morison's formula assumed a fully submersible element. And viscous effects from pontoons and net elements can not be neglected in global response analysis.

2.1.2   Gravity Cage

Zhao et al. [29] developed a numerical model to simulate the dynamic response of the gravity cage under waves and currents. A mesh element is described by a lumped mass model. Mass is concentrated to knot and filaments are modeled by bar elements. In the numerical process, hydrodynamic coefficients for a mesh bar was calculated by empirical formula. Forces on the system was obtained by combining the force on each segment. Physical experiment was conducted and verified the numerical model.

2.1.3   Flexible Cage

Kristiansen and Faltinsen [16] proposed a screen type of force model for viscous hydrodynamic loads on net. They divided the net into flat net panels, which is applicable to any kind of net geometry. Truss element was used to model the net. A circular net in steady current case was studied by numerical methods, and results were compared with the experimental data. A good agreement was reached.

The difference from Kristiansen's model and Ocean Farm 1 is that Kristianse built a flexible model, with large deformation in wave and current, while Ocean Farm 1 is a rigid semi-submersible structure. When fixed on relative dense frames, the net will not have large deformation.

2.2   Net Force Calculation Approaches

Net attached on the structure will bear wave forces and the total force for all net element will be too large to neglect. However, the number of cells in a fishing net could be up to 1 million. Modeling net is not a proper choice considering the computing complexity and

running time. Therefore, it is necessary to propose a method, by which the net force can be transferred to the rigid body.

Forces on the net can be divided into inertia force, tension force, life force drag force, buoyancy and gravity. Considering the mass of a net element will be small and net motion is not violent, the inertia force can be neglected. Two main models for calculating net force are Morison model and screen model.

2.2.1 Morison Model

Morison's equation tells the force normal to the cylinder. Figure 2.1 illustrates the force acting on a cylinder in water. It can not only be applied on the cylinder structures, but also on small elements like riser or net filament. In section 4.1.1, it explained the common used formula for calculation by Morison theory.

(a) Force direction definition   (b) Cross section illustration
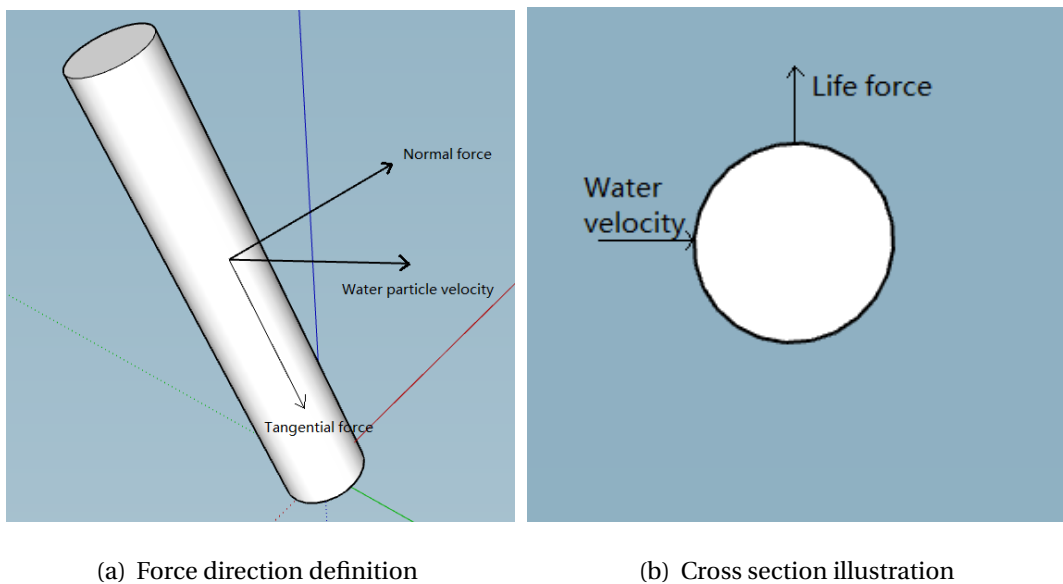
Figure 2.1: Definition of force acting on a cylinder

The original Morison's equation only considered the inertia force and drag force. A mean lift force can be calculated by:

$$F_l = \frac{1}{2} C_l \rho \, d \, A \cdot u_n^2 \tag{2.1}$$

Morison model has a wide use in computation software. But it will over-predict the drag force for large inflow angles on a net panel.

2.2.2 Screen Model

The principle of screen model is to divide the net into several net panels, which can give a good estimation on the total force acting on the net panels. Large inflow angle can be taken into consideration . But it is not commonly used in softwares. To do calculation by screen model, special force coefficients have to be obtained experimentally in advance.

Screen model takes the inflow angle into account and can give a relative accurate result. But it only considers the drag force and lift force. Inertia force should be calculated separately as in Morison's formula. And it can not be applied directly in computing software. Screen model method can be used as a preliminary step before software calculation.

BORE et al.[11] proposed a modified Morison model. To modify the over prediction of drag force for large inflow angles, drag and lift coefficients from screen model are converted into equivalent Morison coefficients. The conversion is simple defined as:

$$C_d = \frac{C_{d,screen}}{Sn_{model}} \tag{2.2}$$

$$C_l = \frac{C_{l,screen}}{Sn_{model}} \tag{2.3}$$

Implementing procedure of modified Morison model were summarized:

- Element unit normal vector to be defined in the same direction as the local net panel normal vector;

- Screen model force coefficients to be estimated either by experimental methods or empirical formulas;

- Solidity ratio to be calculated for the modeled net;

- Coefficients to be converted to Morison coefficients.

The modified Morison model proposed by Bore considered the effect of inflow angle. So it can be applied on net panel facing in different direction. And the simplification concept of modeling the fish farm can be referred to when building geometry model.

2.2.3   Other Methods for Net Force Calculation

Some other approaches for calculating net force have been proposed and applied.

Tsukrov and Eroshkin [28] proposed a consistent finite element, which can reproduce drag force, buoyancy, inertial force, and elastic forces. The concept was applied on FEM program and results were compared with semi-empirical formula of KawaKami (1959,1964). Finally, the approach was applied on a tension leg fish cage with results compared with equivalent truss element model, which showed enough accuracy.

The theory behind is to substitute dense mesh elements with one element with larger size, which has same hydrodynamic and elastic properties. IF the consistent element has a size, which is realizable to build in modeling, this method could be a good way to simulate the mesh effect. However, as the consistent element goes to a larger size, the similarity to real hydrodynamic properties will become worse. So the limitation of this approach is obvious.

Huang and Tang [13] divided the net cage into plane surface elements based on lumped mass method. Drag and lift force on net was calculated by Løland formula. Inertia force was expressed with local acceleration at the center of a net element. Tension force was assumed to act only between neighboring nodes. With the external forces above defined, the forces were evenly distributed on nodes of a net element. The numerical results were validated by a physical test, which showed that the accuracy depends on Reynolds number. With Reynolds number lower that suggested range, the numerical method would under-predict the external force.

Moe-Føre and Christian [20] evaluated three numerical model based on springs, trusses and triangular finite elements. Spring model implemented a nonlinear formulation of spring stiffness and included wake effects. Truss method applied 3D truss element to model the net. Joint effects and tangential force were neglected. Triangle method modeled the net with triangular elements, which didn't carry compressive loads. The results showed that triangle model overestimated the net deformation. For drag and lift force, spring and truss model gave a similar result, while the triangle model showed a change in slope. Overall, it concluded that the three numerical methods can gave a load and deformation estimation within an acceptable tolerance limit and the accuracy depends on hydrodynamic coefficents.

11

Chapter 3

Ocean Farming 1 Concept

3.1   Concept Description

The modeling object is Ocean Farm 1, which is an offshore project by SalMar. A basic configuration of Ocean Farm 1 is shown in figure 3.1. The main structure consists of 12 side columns and 1 central column with central pontoon. There is a side pontoon on every second side column, which is designed to provide sufficient stability when facing severe sea states.

The mooring system consists of 8 catenary lines,as used on oil platforms. With 2 lines in a group, all catenary lines are fixed on 4 floating elements.[12]. As it can be seen, besides the steel parts, the structure also includes sensors, cameras, and a control room as a personnel living quarter.

Considering the suitable biological condition for fish, the farm is designed to operate for water depths of 100 to 300 meters. It is also equipped with one movable and two fixed bulkheads to divide the volume into 3 compartments, so that different operations can be performed without interactions [21].

The fish cage has now arrived at Frohavet, which is the sea area between Fosenhalvøya and the archipelago of Froan in Sør-Trøndelag. Water depth at the site is taken as 150 meters. Sintef did a model test for Ocean Farm 1 under realistic sea-states with waves, current and wind conditions similar to those experienced at Frohavet Sea, including maximum wave heights of almost 10 m [8].
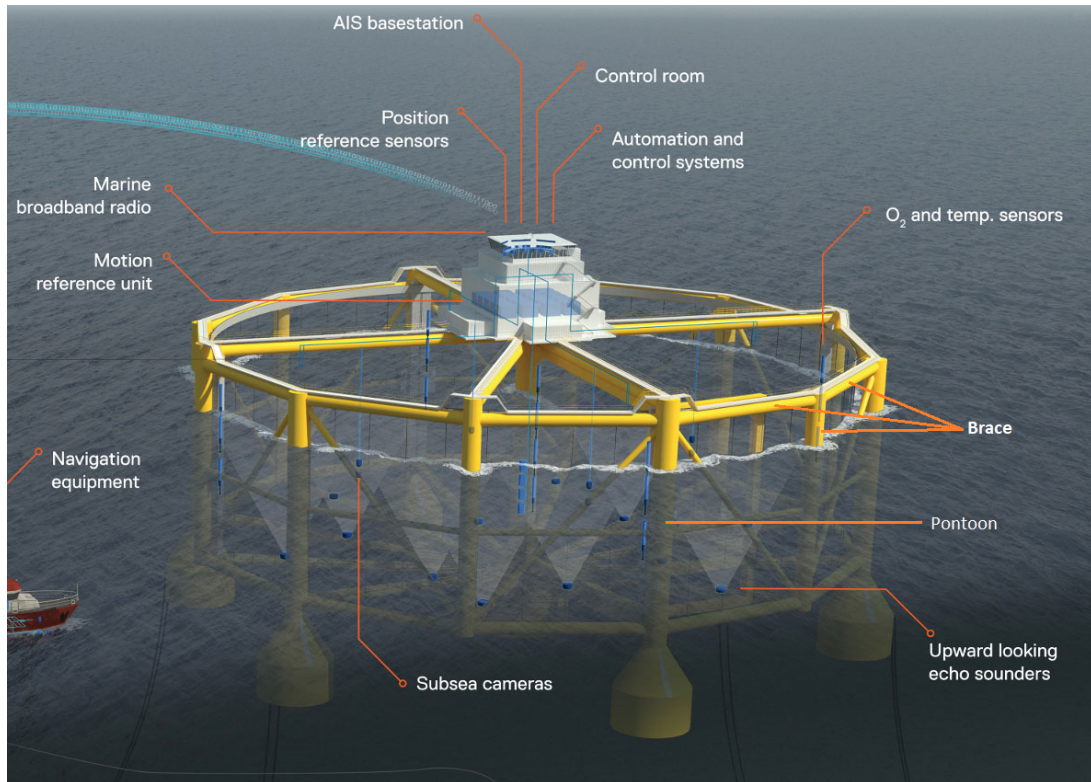
Figure 3.1: Ocean Farm 1 configuration [9]

3.2 Technical Information

The main dimensions of Ocean Farm 1 is summarized in figure table 3.1. It is relatively large structure compared conventional cages. The expected number of fish allowed in a net cage is around 200 000. [19]

Table 3.1: Parameters of Ocean Farm 1 [23]

Dimension	Unit	Value
Overall height	[m]	67
Diameter	[m]	110
Circumference	[m]	341.6
Volume	[m^3]	245,000
Weight	[$tonnes$]	5600
Operation draft	[m]	43

The construction material is NV-36 steel, properties of which are listed in table 3.2.

Table 3.2: material properties of main structure [23]

Property	Symbol	Unit	Value
Young's Modulus	E	$[GPa]$	210
Yield strength	σ_y	$[MPa]$	355
Poisson's ratio	v	$[-]$	0.3
Density	ρ	$[kg/m^3]$	7850

3.3 Mooring System

The mooring system consists of 8 1100-meter-long catenary lines, with a 45 degree angle between each two lines. The catenary lines is made of chain but with a fiber rope at the top. Properties of the two materials of catenary line are shown in table 3.3.

Table 3.3: Properties of the mooring lines [23]

Property	Unit	Chain	Fiber
Length	$[m]$	1000	100
Diameter	$[mm]$	88	160
Axial stiffness	$[MN]$	680.81	235.44
Minimum breaking load	$[kN]$	7051.4	8122.7
Submerged weight	$[kg/m]$	147	4.0

3.4 The Cage Net

The net is stretched over the sides and bottom. The net type applied on Ocean Farm 1 is EcoNet, which is a non-fiber material with hard surface that resists marine fouling. It is stiffer than tradition net fibers, as well as lower weight. A mesh unit of Econet is illustrated in figure 3.4 .
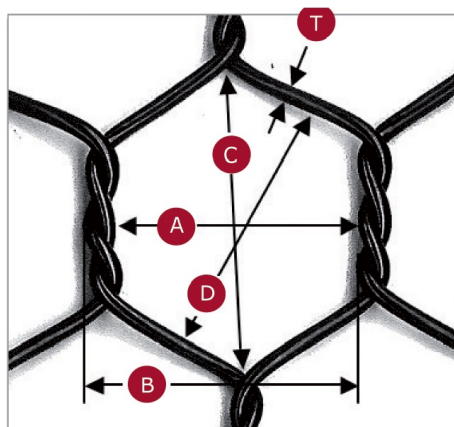
- A = Mesh width
- B = Mesh pitch
- C = Mesh height
- D = Mesh diagonal
- T = Wire thickness

Figure 3.2: Illustration of a single mesh of small-size EcoNet [10]

Econet has three mesh size. The net used in Ocean Farm 1 has small size mesh. Numbers of small size mesh are given in table 3.4.

Table 3.4: Dimension of small-size Econet [10]

Mesh size	t(mm)	A(mm)	B(mm)	C(mm)	D(mm)	Weight(g/m^2)
Small:	2.5	35	40	43	37	570

Chapter 4

Theoretical Background

4.1 Environmental Loads

The determination of environment loads is the first step for analysis. Generally the loads are from wind, wave and current. As the projected area in wind is small, wind load is not considered in the analysis. Two aspects of theory, wave load and current load are explained in this section. Most of the formulas and coefficients determinations are based on DNVGL guidebook [24].

4.1.1 Wave Theory

Deep Water Assumption

Global maritime has evaluated the sea states in Frohavet sea. An estimation of 100-year current velocity is, $U_{C,100}$ = 0.75 m/s and 100-year wave condition, with annual probability of occurrence of 0.01, is a combination of wave height H_S = 5m and zero-crossing period T_z = 11s. Wave length under such wave period can be calculated as:

$$\lambda = \frac{g T^2}{2\pi} = 188 \quad \text{m} \tag{4.1}$$

Deep water condition is assumed when water depth at the site is larger than half of wave length. With water depth

$$h = 150m > \frac{1}{2} \times 188 = 94m \tag{4.2}$$

Therefore, the criterion of deep water assumption is fulfilled.

Dispersion relation for deep water is

$$k = \frac{\omega}{g} \tag{4.3}$$

Regular Wave Theory

Potential theory for regular waves is applied in this thesis. Basic assumptions are made in potential theory [22].

Sea water is assumed incompressible and inviscid. Fluid motion is assumed irrotational. The velocity potential satisfies Laplace equation

$$\frac{\partial^2 \phi}{\partial x^2} + \frac{\partial^2 \phi}{\partial y^2} + \frac{\partial^2 \phi}{\partial z^2} = 0 \tag{4.4}$$

Consider boundary conditions

$$\frac{\partial \zeta}{\partial t} = \frac{\partial \phi}{\partial z} \quad \text{on } z = 0 \quad \text{kinematic condition} \tag{4.5}$$

$$g\zeta + \frac{\partial \phi}{\partial t} = 0 \quad \text{on } z = 0 \quad \text{kinematic condition} \tag{4.6}$$

Wave potential for deep water can be solved to

$$\phi = \frac{g\zeta_a}{\omega} e^{kz} \cos(\omega t - kx) \tag{4.7}$$

Wave elevation is expressed as

$$\zeta = \zeta_a \sin(\omega t - kx) \tag{4.8}$$

Velocity in x and z components can be derived from wave potential:

$$u = \omega \zeta_a e^{kz} \sin(\omega t - kx) \tag{4.9}$$

$$w = \omega \zeta_a e^{kz} \cos(\omega t - kx) \tag{4.10}$$

4.1.2 Morison Theory

Wave loads is the main component of environment factors for semi-submersible structures. As the submerged part consists of cylindric pontoons, the wave load can be calculated by Morison's load model if the following requirement is met:

$$\lambda > 5D \tag{4.11}$$

where

λ is the wave length;

D is the diameter of the member.

For a moving structure in waves and current, the load can be calculated by

$$f_N(t) = -\rho C_A A\ddot{r} + \rho(1 + C_A)A\dot{v} + \frac{1}{2}C_D Dv|v| - \frac{1}{2}C_d D\dot{r}|\dot{r}| \tag{4.12}$$

where

f_N is the sectional force;

ρ is the mass density of water;

C_A is the added mass coefficient;

C_D is the drag coefficient;

C_d is the hydrodynamic damping coefficient;

A is the cross-section area;

v is the wave velocity;

$\dot{v}$ is the wave acceleration;

$\dot{r}$ is the velocity of member normal to axis;

$\ddot{r}$ is the acceleration of member normal to axis.

Added Mass Coefficient

Added mass coefficient is defined as:

$$C_A = \frac{m_a}{\rho A} \tag{4.13}$$

It can be determined by KC number, which is defined as:

$$K_C = v_m T / D \qquad (4.14)$$

where

T is the wave period of oscillation;

v_m is the maximum orbital particle velocity;

For $K_C < 3$, C_A can be equal to 1. For drag force is the dominating force, $K_C > 3$, C_A can be determined by:

$$C_A = max \begin{cases} 1.0 - 0.044(K_C - 3) \\ \\ 0.6 - (C_{DS} - 0.65) \end{cases} \qquad (4.15)$$

where $C_{DS} = 0.65$ for smooth surface, and $C_{DS} = 1.05$ for rough cylinder.

Figure 4.1 shows the variation of C_A with K_C, where solid line is used for smooth surface cylinder and dotted line for rough surface cylinder.
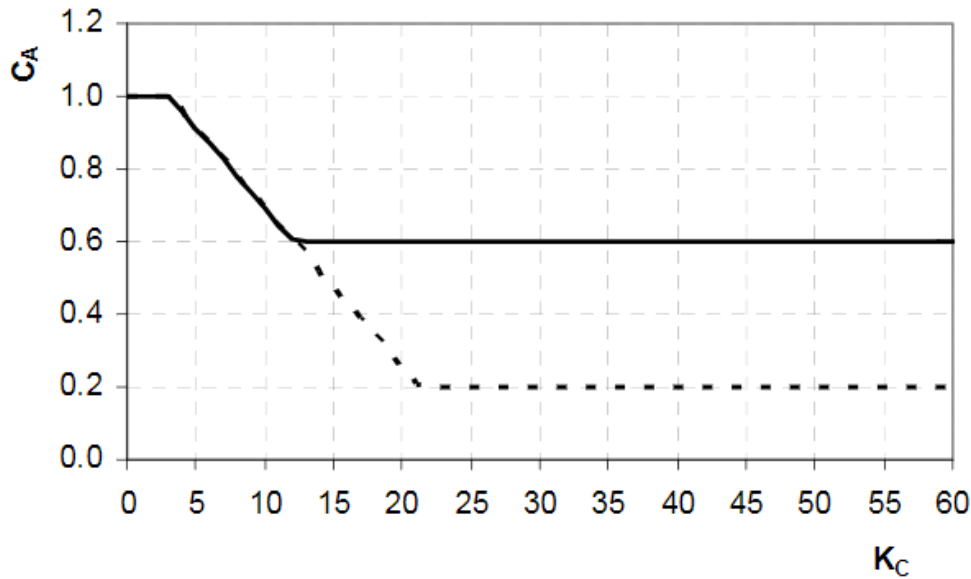

Figure 4.1: Added mass coefficient for circular cylinder [24]

For simplification, KC in this thesis study takes the value around 3 and the structure is treated as rough surface. Thus C_A takes the value of 1 for all main structures. While for mooring lines, the surface is treated as smooth and $C_A = 0.2$.

Drag Coefficient

The drag coefficient is defined as:

$$C_D = \frac{f_{drag}}{\frac{1}{2}\rho D v^2}$$ (4.16)

It can be determined by Reynolds number and surface toughness as shown in figure 4.2.
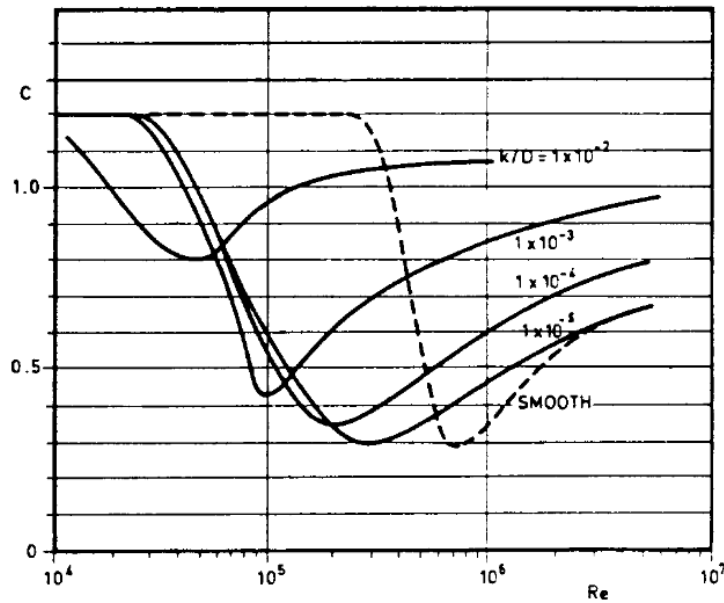

Figure 4.2: Drag coefficient for circular cylinder [24]

In this thesis, for steel components, C_D = 0.8. For mooring lines, C_D = 2.4 for the chain part and 1.6 for the fiber part.

4.1.3 Screen Model Theory

Screen model in principle is a generalization of screen method by Løland [18]. Drag and lift coefficients are defined as functions of solidity ratio and attack angle.

Solidity Ratio

Solidity ratio is the ratio of area projected by the threads of a screen to the total area of the net panel. For a square net as shown in figure 4.1.3, solidity ratio S_n is:

$$Sn = \frac{2d_w}{l_W} - (\frac{d_w}{l_w})^2$$ (4.17)

21

where

d_w is the diameter of twine;
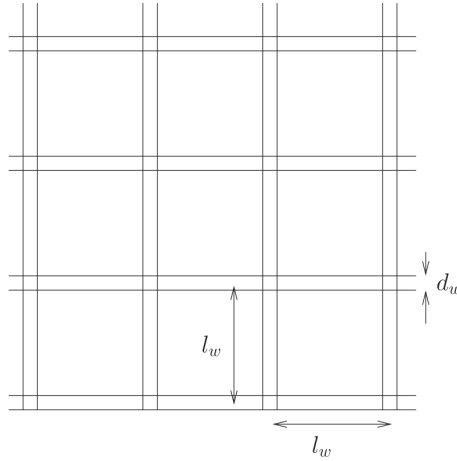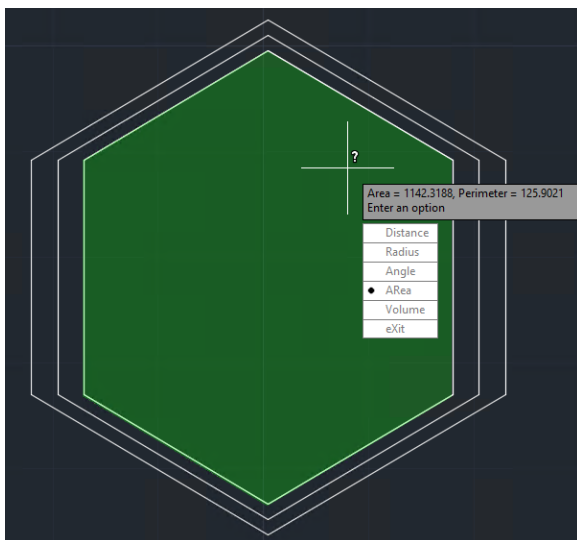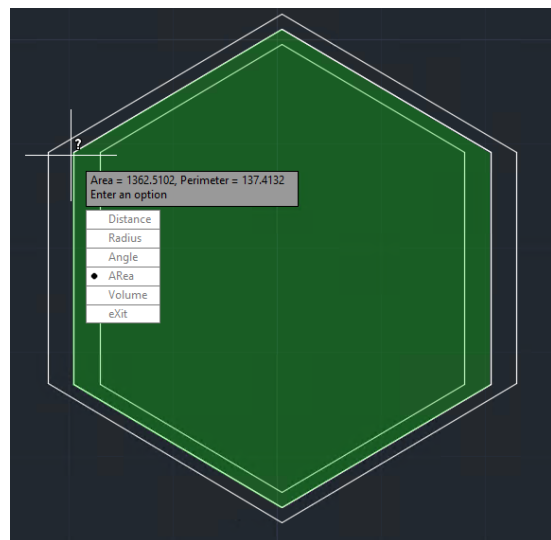
l_w is the length of twine

Figure 4.3: Illustration of net twine

For hexagon mesh of Econet, as shown in figure 3.4, solidity ratio is calculated with the same principle. 2D drawing of a net mesh is made in AutoCAD and the inner and outer area are calculated automatically, as shown in figure 4.1.3.

(a) Inner area
(b) Outer area

Figure 4.4: Illustration of solidity ratio calculation

Outer area minus inner area gives the area of threads:

$$A_{thread} = A_{out} - A_{in} = 1362.51 - 1142.32 = 220.19 \quad m^2 \tag{4.18}$$

Solidity ratio of the net cage on Ocean Farm 1 is:

$$Sn = \frac{A_{thread}}{A_{out}} = \frac{220.19}{1362.51} = 0.162 \tag{4.19}$$

Force Calculation in Screen Model

Drag and lifting force in screen model acting on a net panel can be calculated as:

$$F_{d,screen} = \frac{1}{2}C_{d,screen}(\theta)A' \cdot U_{rel}^2 \tag{4.20}$$

$$F_{l,screen} = \frac{1}{2}C_{l,screen}(\theta)A' \cdot U_{rel}^2 \tag{4.21}$$

where

A' is the area of the net panel;

U_{rel} is the relative inflow velocity;

θ is the angle between relative inflow direction and the net normal vector in the direction of the flow, as defined in figure4.5;
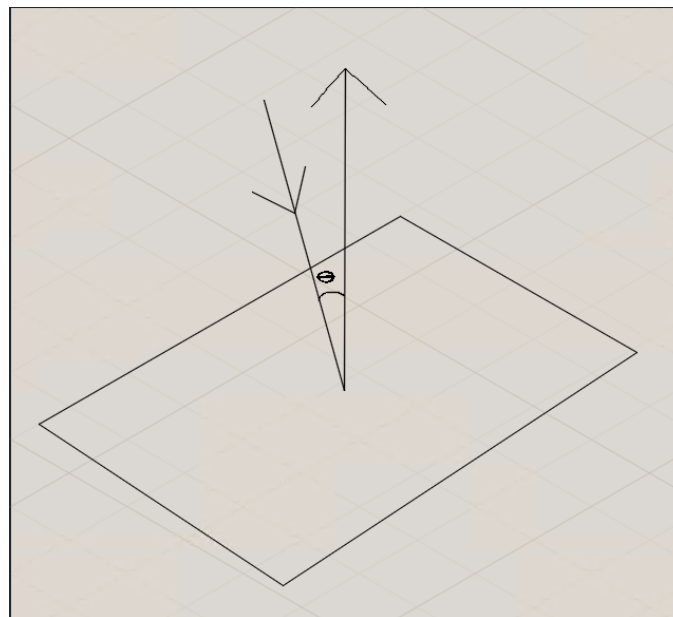

Figure 4.5: Definition of θ

$C_{d,screen}$ and $C_{l,screen}$ are drag and lift coefficients of the screen panel, which are primarily determined by experiments.

Løland has estimated a drag and lift coefficient formula, known as Løland formulas:

$$C_{d,screen}(\theta) = 0.04 + (-0.04 + 0.33Sn + 6.54Sn^2 - 4.88Sn^3)\cos(\theta) \tag{4.22}$$

$$C_{l,screen}(\theta) = (-0.05n + 2.3Sn^2 - 1.76Sn^3)\sin(2\theta) \tag{4.23}$$

4.1.4 Current Load

Current load can take the same method as wave load calculation in eq. (4.12). But v and $\dot{v}$ are defined as velocity and acceleration of current. Denote the surface current velocity as U, divided into the following components [22]:

$$U = U_t + U_w + U_s + U_m + U_{set-up} + U_d \tag{4.24}$$

where

U_t is the tidal component;

U_w is the component generated by local wind;

U_s is the component generated by Stokes drift for regular waves;

U_m is the component from major ocean circulation, which depends on geographical location;

U_{set-up} is the component due to set-up phenomena and storm surges;

U_d is the local density-driven current governed by strong density jumps in the upper ocean.

4.2 Motion Analysis

4.2.1 The Equation of Motion

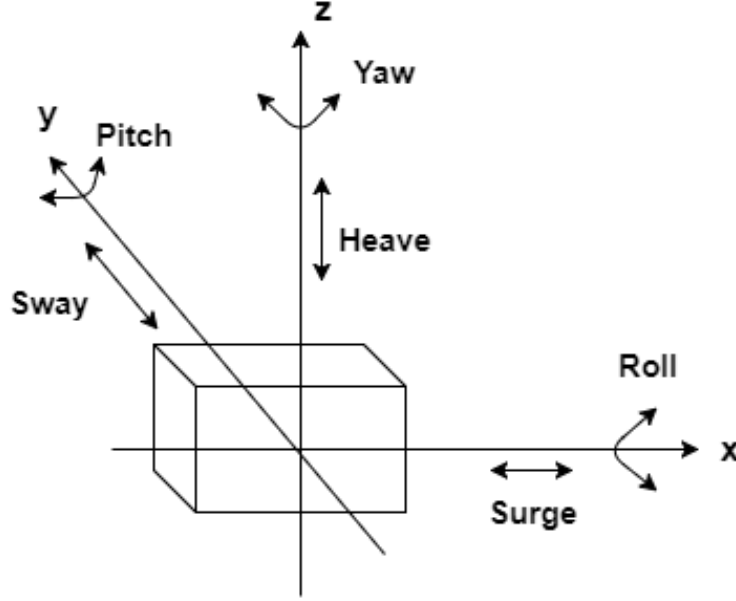Motions under 6 degrees of freedom for offshore structures are defined as figure 4.6.

Figure 4.6: Motion definition of offshore structures

Rigid body motions can be expressed as:

$$\sum[(M_{jk} + A_{jk})\ddot{\eta}_k + B_{jk}\dot{\eta}_k + C_{jk}\eta_k] = F_j e^{-i\omega_e t} \tag{4.25}$$

where

M_{jk} are the components of the generalized mass matrix for the structure;

F_j are the complex amplitudes of the exciting forces and moment;

For structure with lateral symmetry, the coupling is weak between dof(1,3,5) and dof(2,4,6).The six coupled equations will reduce to two sets of equations, one set for surge, heave and pitch and the other for sway, roll and yaw as

$$\left\{ \begin{bmatrix} m & 0 & mz_G \\ 0 & m & 0 \\ mz_G & 0 & I_{55} \end{bmatrix} + \begin{bmatrix} A_{11} & A_{13} & A_{15} \\ A_{31} & A_{33} & A_{35} \\ A_{51} & A_{53} & A_{55} \end{bmatrix} \right\} \begin{bmatrix} \ddot{\eta}_1 \\ \ddot{\eta}_3 \\ \ddot{\eta}_5 \end{bmatrix} + \begin{bmatrix} B_{11} & B_{13} & B_{15} \\ B_{31} & B_{33} & B_{35} \\ B_{51} & B_{53} & B_{55} \end{bmatrix} \begin{bmatrix} \dot{\eta}_1 \\ \dot{\eta}_3 \\ \dot{\eta}_5 \end{bmatrix} + \begin{bmatrix} 0 & 0 & 0 \\ 0 & C_{33} & C_{35} \\ 0 & C_{53} & C_{55} \end{bmatrix} \begin{bmatrix} \eta_1 \\ \eta_3 \\ \eta_5 \end{bmatrix} = \begin{bmatrix} F_{10}\cos(\omega_e + \epsilon_1^F) \\ F_{30}\cos(\omega_e + \epsilon_3^F) \\ F_{50}\cos(\omega_e + \epsilon_5^F) \end{bmatrix} \tag{4.26}$$

$$\left\{ \begin{bmatrix} m & -mz_G & 0 \\ -mz_G & I_{44} & I_{46} \\ 0 & I_{64} & I_{66} \end{bmatrix} + \begin{bmatrix} A_{22} & A_{24} & A_{26} \\ A_{42} & A_{44} & A_{46} \\ A_{62} & A_{64} & A_{66} \end{bmatrix} \right\} \begin{bmatrix} \ddot{\eta}_2 \\ \ddot{\eta}_4 \\ \ddot{\eta}_6 \end{bmatrix} + \begin{bmatrix} B_{22} & B_{24} & B_{26} \\ B_{42} & B_{44} & B_{46} \\ B_{62} & B_{64} & B_{66} \end{bmatrix} \begin{bmatrix} \dot{\eta}_2 \\ \dot{\eta}_4 \\ \dot{\eta}_6 \end{bmatrix} + \begin{bmatrix} 0 & 0 & 0 \\ 0 & C_{44} & 0 \\ 0 & 0 & 0 \end{bmatrix} \begin{bmatrix} \eta_2 \\ \eta_4 \\ \eta_6 \end{bmatrix} = \begin{bmatrix} F_{20}\cos(\omega_e + \epsilon_2^F) \\ F_{40}\cos(\omega_e + \epsilon_3^F) \\ F_{60}\cos(\omega_e + \epsilon_6^F) \end{bmatrix} \tag{4.27}$$

For a semi-submersible pontoon as shown in figure 4.2.1, two degrees of freedom of interest for the structure are heave and pitch. These two motion analysis are to be explained more
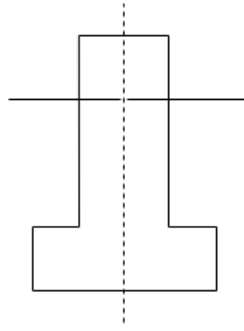
detailedly.

Figure 4.7: Semi-submersible pontoon model

Assume the wave is in beam sea direction, the undamped equation of motion for heave and pitch can be written as:

$$(M + A_{33})\frac{d^2\eta_3}{dt^2} + C_{33}\eta_3 = F_3(t) \tag{4.28}$$

$$(I_5 + A_{55})\frac{d^2\eta_3}{dt^2} + C_{55}\eta_5 = F_5(t) \tag{4.29}$$

4.2.2 Transfer Function

Transfer function, or names as response amplitude operator(RAO), is used to predict the response of a platform under sea state. It is defined as the response amplitude over the wave amplitude, as:

$$Y(\omega) = \frac{\eta_{k0}}{\zeta_0} \tag{4.30}$$

As the transfer function is based on frequency domain, a resonance frequency can be intuitively reflected.

4.3 Summary

In this chapter, theories applied for the calculation are described. Environmental load mainly covers wave and current. How these loads act on the structure are explained and formulas are given. Motion equation of 6 dof coupling effect are introduced. Finally, calculation approach in frequency domain as transfer function is briefly interpreted.

Some results calculated in this chapter are summarized below.

Table 4.1: Sea state information summary

Property	Symbol	Unit	Value
Current velocity	U_C	[m/s]	0.75
Wave height	H_S	[m]	5
Wave period	T_P	[s]	11
wave frequency	ω	[rad/s]	0.57
Wave length	λ	[m]	188
Wave number	k	[-]	0.033

Table 4.2: Hydrodynamic coefficients summary

Property	Symbol	Chain	Fibre	Main structure
Drag coefficient	C_D	2.4	1.6	0.8
Added mass coefficient	C_A	0.2	0.2	1
Inertia coefficient	C_M	1.2	1.2	2

Table 4.3: Cage net information summary

Property	A_{in}	A_{out}	A_{thread}	Sn
Value	1142.32 $[mm^2]$	1362.51 $[mm^2]$	220.19 $[mm^2]$	0.162

Determination of environmental loads is the first step of the calculation for both motion analysis and stress analysis. Environment loads should be taken from the operation site statistics, which can be applied with some proper assumption and approximation for a calculation simplicity. Motion response are to be analyzed in time domain.

Chapter 5

Modeling and Numerical Calculation

5.1 FEM Modeling

To model the structure as correctly as possible, dimensions of crucial parts should be kept same as the real structure. Figure 5.1 and table 5.1 show the illustration of a complete structural parts and dimensions of main components.
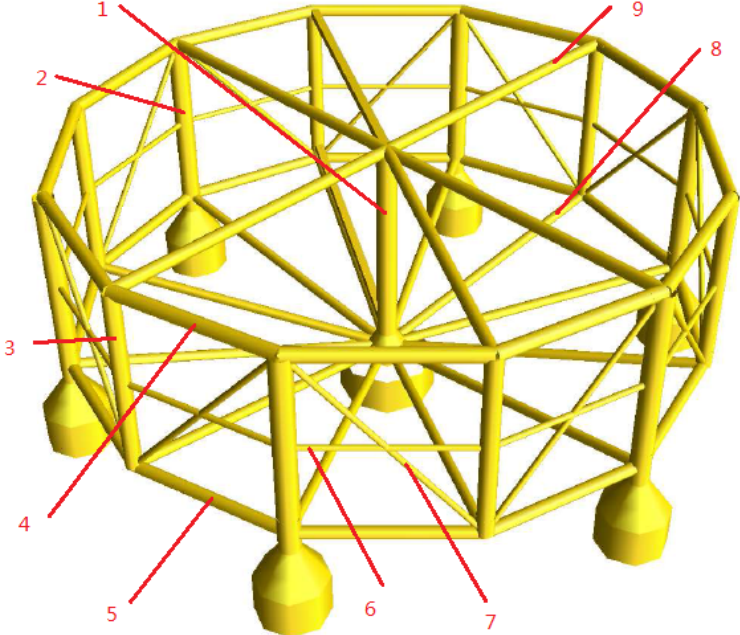

Figure 5.1: Illustration of the model [23]

Table 5.1: List of dimensions of all the parts of the structure

Number	Segment	Diameter [m]	Thickness [mm]
1	Center column and pontoon	3.56	32
2	Side column with pontoon	3.56	34
3	Side column without pontoon	2.8	30
4	Top outer ring beams	2.29	18
5	Bottom outer ring beams	2.05	24
6	Mid outer ring beams	1	15
7	Mid outer diagonal beams	1	15
8	Bottom radial beams	1.75	23
9	Top cross beam	2.05	18

5.1.1 Panel Model

Parts with larger dimension are to be built as panel model. Analysis in HydroD has a maximum limit of panel elements as 15000, which means the number of mesh should be no more than 15000. Considering the wave length is about 40-150m, the element size should be less than $40/6 \approx 7$m. To check the mesh size applicability, node number and element size for main parts are calculated, as listed in table 5.2.

Table 5.2: Summary of mesh size of main parts

Segment	Total length [m]	NO. of element	Element length [m]
center column	31	8	3.87
side column	26	7	3.7
Bottom radial beam	48	15	3.2
Bottom outer ring	23	6	3.83

In order to smoothly mesh a edge, the number of element is taken as 10 for a cross section. To give a fine mesh, two meshing methods are applied. One is by setting node number along the edge and the other is by directly setting mesh size. Quad mesh element with large length-width ratio is applied. Finer element are used around the joint to have a better detail
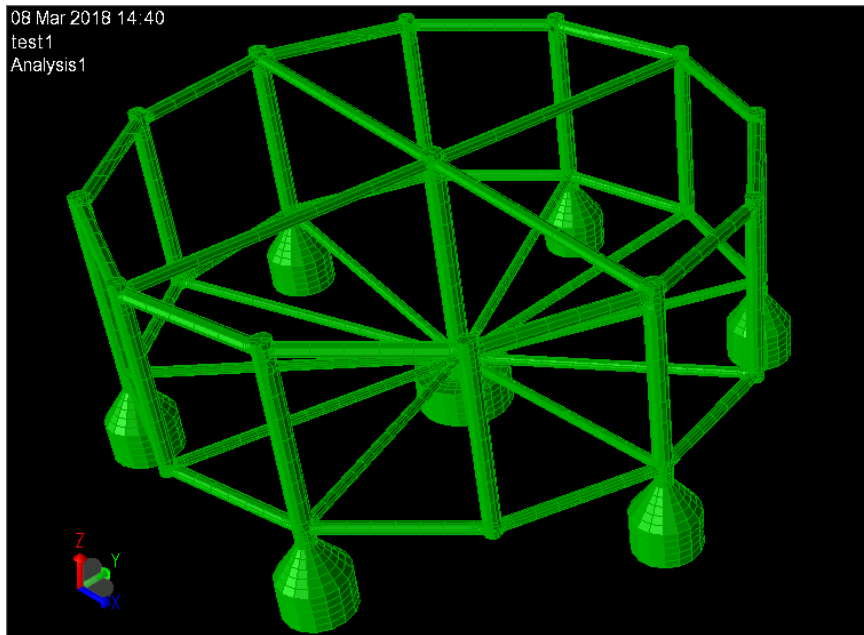
modeling. Figure 5.2 and 5.3 illustrates the general and local FEM model in GeniE respectively.
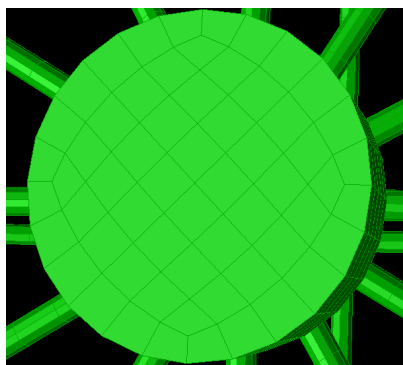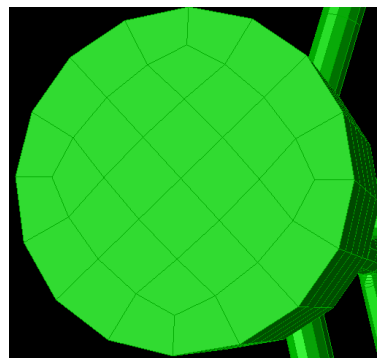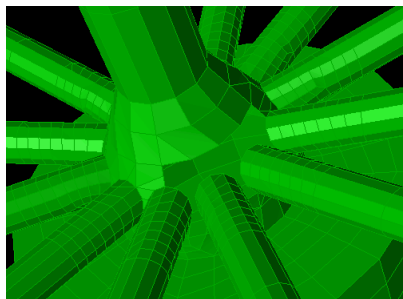

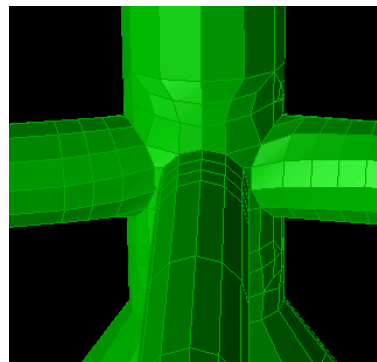Figure 5.2: FEM panel model

(a) Bottom of central pontoon

(b) Bottom of side pontoon

(c) Joint around central cone

(d) Joint around side cone

Figure 5.3: Detail FEM illustration at joints

When considering further force calculation on modeled structure, special attention should be paid.

The real wave force acting on panel elements includes two parts:

$$dF = \rho(1 + C_A)a_w \cdot A \cdot dl + \frac{1}{2}\rho \cdot C_D \cdot v_w|v_w| \cdot D \cdot dl$$

The first term on the right side represents the inertia force and the second term represents drag force. Panel element takes only inertia part into account. To give an accurate description, drag force acting on these parts should be modeled separately. In this thesis, the proposed approach is to include the drag force by build a Morison model. To avoid the inertia term in Morison element being repeated calculated, the diameter of the objected is scaled by 0.001, while hydrodynamic coefficients, C_A and C_D are scaled by 1000.

5.1.2 Morison Model

The Morison model is built, including the rest slender structure components and drag effect of larger parts, as shown in figure 5.4 below. Hydrodynamic coefficients of the Morison model are defined in HydroD.
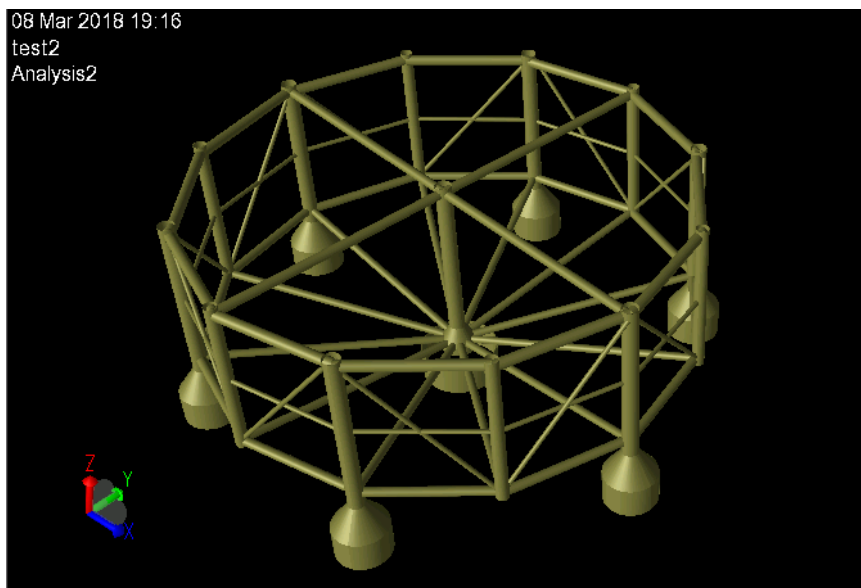

Figure 5.4: Illustration of Morison model

5.1.3 Mass Model

For a good estimation of mass distribution, a beam model for all components (T3.FEM) should be build with respective wall thickness and density. Mass of the steel structure are built by setting an appropriate cross-section and density of each component.

Ballast are taken into consideration by calculating a average density of ballast and steel.

$$\rho' = (\rho_{sw} * V_{ballast} + \rho_{st} * V_{steel}) / V_{steel'}$$

where V_{steel} is the steel volume below the ballast free surface, including the pontoon bottom plate, while $V_{steel'}$ only represents the side, as described by beam element.

The filling ratio of each pontoon and average density are calculated, as listed in table 5.3.

Table 5.3: Filling ratio of ballast

Pontoon	Filling ratio [%]	Free surface position [m]	Average density [kg/m^3]
C2,C4,C6 cylinder	88.6	9.132	5.601e+04
C8 cylinder	89.2	9.238	5.582e+04
C10 cylinder	82.9	8.263	5.761e+04
C12 cylinder	83.9	8.4	5.735e+04
Mid cylinder	37.7	2.971	5.02e+04

Besides the mass from main structure and ballast, other mass contributions from upper-structure, bulkhead and equipments are represented as node mass, which is built as point mass in GeniE. Nodel mass distribution are summarized in table 5.4.

Table 5.4: Nodal mass distribution

Contribution	Weight [kg]	Number of Nodes	Z-position [m]
Upper-structure	350496	1	60
Fixed bulkhead	172001	10	16, 39
Movable bulkhead	195706	5	39
Others	1969591	12	31

The final mass model with point mass are shown in figure 5.5. Some important parameters

related to mass are compared with Global maritime, given in Bore's article[23], as shown in table 5.5. Since net is not considered at the moment, the total weight of FEM model is slightly lower than that of real structure.

Table 5.5: Mass comparison

Property	Mass model	Global Maritime	Unit
Total weight	14157	16325	[tonne]
VCG(from baseline)	17.11	17.94	[m]
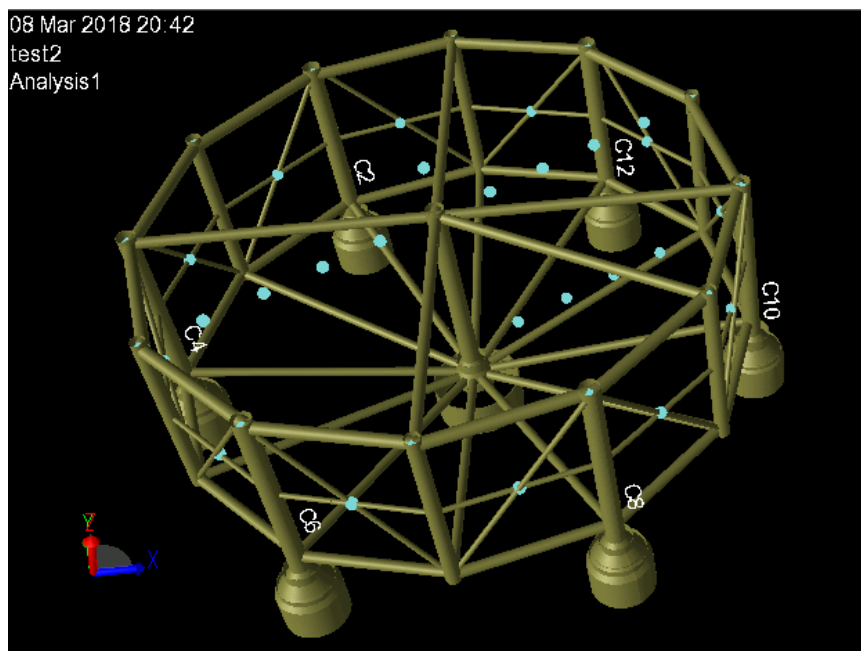
Figure 5.5: Mass model

5.2 Frequency Domain Hydrodynamic Calculation

With FEM model input into HydroD, hydrodynamic calculations can be made. Results of mass matrix, damping matrix and RAO of 6 dof motions are printed below.

5.2.1 Mass Matrix

- Added mass matrix at frequency 0.7.

9.565E+06	1.941E+04	-2.235E+04	6.261E+05	-2.692E+08	-9.826E+03
1.017E+04	9.564E+06	2.219E+04	2.691E+08	-4.300E+05	-1.212E+04
-2.772E+04	2.774E+04	8.449E+06	9.938E+05	9.783E+05	1.043E+05
3.373E+05	2.692E+08	8.196E+05	1.713E+10	-1.510E+07	-1.692E+04
-2.692E+08	-7.360E+05	8.100E+05	-2.437E+07	1.713E+10	5.826E+05
-1.829E+04	-1.592E+04	5.243E+04	-6.945E+05	1.263E+06	2.160E+10

- Body mass matrix.

1.458E+07	0.000E+00	0.000E+00	0.000E+00	-3.775E+08	-7.141E+06
0.000E+00	1.458E+07	0.000E+00	3.775E+08	0.000E+00	-8.074E+04
0.000E+00	0.000E+00	1.458E+07	7.141E+06	8.074E+04	0.000E+00
0.000E+00	3.775E+08	7.141E+06	3.278E+10	1.669E+08	-1.391E+08
-3.775E+08	0.000E+00	8.074E+04	1.669E+08	3.255E+10	-1.033E+08
-7.141E+06	-8.074E+04	0.000E+00	-1.391E+08	-1.033E+08	3.504E+10

5.2.2 Damping Matrix

- Potential damping.

2.110E+02	3.273E+01	-3.865E+02	2.438E+03	-1.010E+05	4.398E+02
-5.254E+01	2.187E+02	3.914E+02	1.027E+05	-1.440E+03	-4.145E+02
-6.942E+02	7.142E+02	1.247E+04	2.814E+04	2.784E+04	-1.472E+04
-2.422E+04	1.202E+05	2.273E+04	6.528E+07	4.977E+05	4.767E+03
-1.191E+05	-3.221E+04	2.256E+04	-9.893E+05	6.526E+07	-1.671E+04
4.087E+01	1.697E+01	-4.981E+02	2.057E+04	-1.219E+04	2.561E+05

- Viscous damping.

7.730E+05	-3.935E-03	-3.235E-04	-7.814E+03	-1.738E+07	-9.857E+05
-8.331E-04	7.730E+05	5.177E-04	1.738E+07	-7.814E+03	5.992E+00
-6.471E-05	5.177E-04	5.403E+05	-6.142E-02	-6.087E-01	1.563E+04
-7.814E+03	1.738E+07	-6.142E-02	1.028E+09	4.221E+00	-3.146E+01
-1.738E+07	-7.814E+03	-6.087E-01	4.221E+00	1.028E+09	1.381E+07
-9.857E+05	5.992E+00	1.563E+04	-3.146E+01	1.381E+07	1.620E+09

5.2.3   Transfer Function

Transfer function in frequency domain of 6 dof motion are presented in figure 5.2.3.

Table 5.6 shows the natural period values from model experiments by MARINTEK[23] and corresponding natural frequencies are calculated.

Table 5.6: Natural periods and frequencies from MARINTEK

Motion	Natural period [sec]	Natural frequency [rad/s]
Surge	175	0.03
Sway	175	0.03
Heave	25.5	0.246
Roll	29	0.217
Pitch	30.8	0.204

From figure 5.2.3, natural frequencies can be roughly estimated from the peak values, as listed in table 5.7.

Table 5.7: Natural frequency from RAO results

Motion	Heave	Roll	Pitch
Natural frequency [rad/s]	0.2	0.16	0.15

There is a difference comparing the two group of natural frequency. The main reason is that the model in MARINTEK has a small pontoon size, which leads to higher natural frequencies. Therefore, the modeling in this thesis is seen accurate enough.
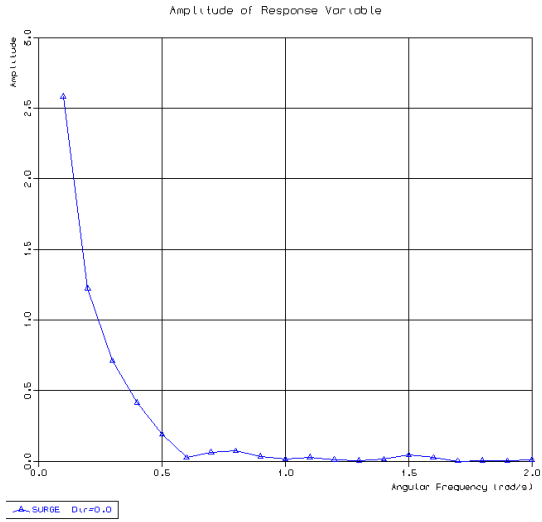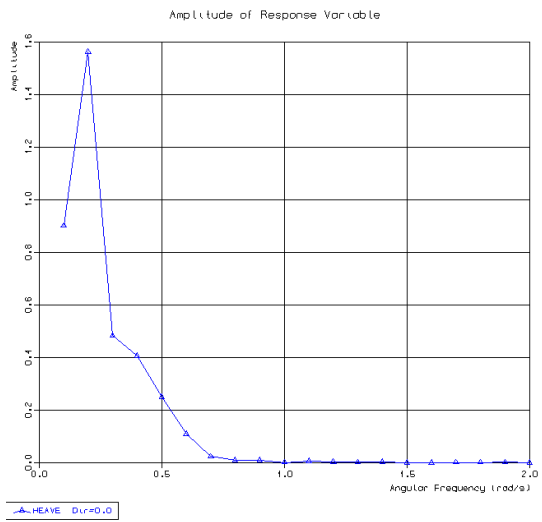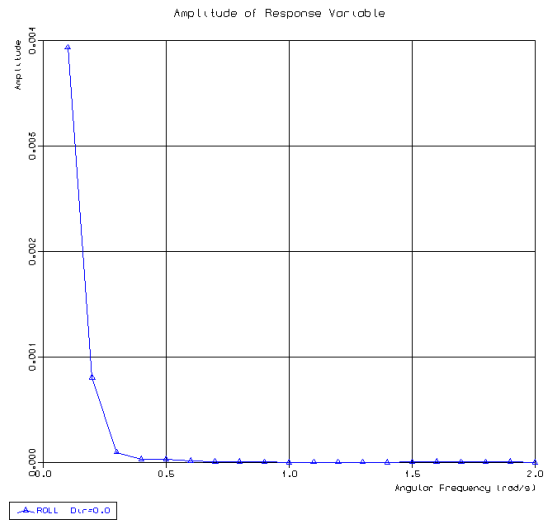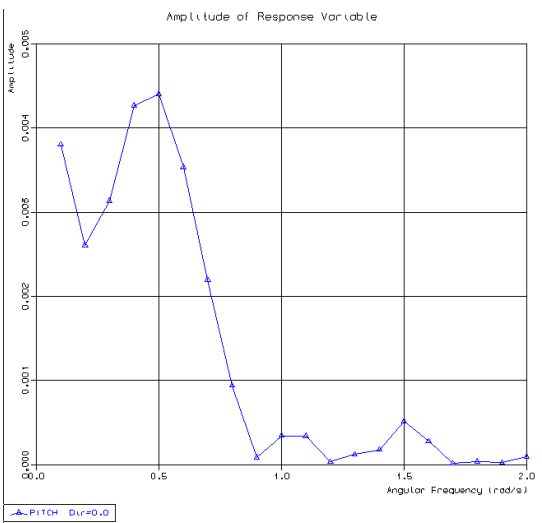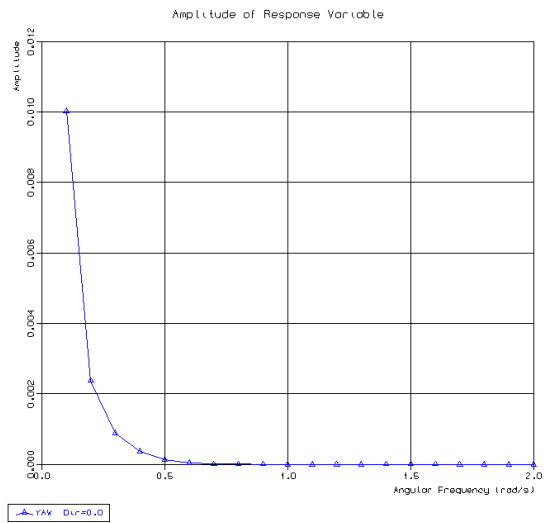
(a) Surge
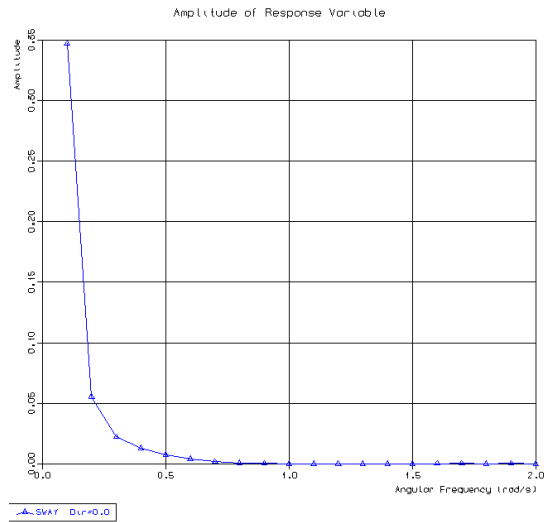
(b) Sway

(c) Heave

(d) Roll

(e) Pitch

(f) Yaw

5.3 Time Domain Response Calculation

5.3.1 Slender Elements

As G1. file from HydroD only contains information for inertia force, the drag force part should be included separately in time domain analysis. The solution in SIMA is to rebuild the Morison model with slender elements.

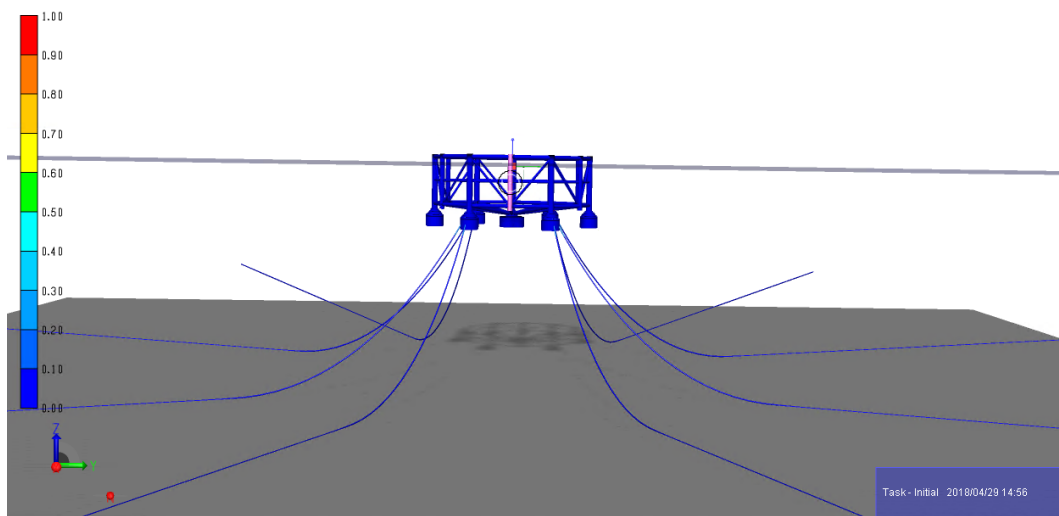The complete slender element model in SIMA with mooring system is shown in figure 5.6.

Figure 5.6: Complete model in SIMA

5.3.2 Mooring System Modeling

Besides the original information about mooring lines listed in table 3.3, the following material information applied in SIMA settings is also required.

Table 5.8: Properties of the mooring lines used in SIMA settings

Property	Unit	Chain	Fiber
Equivalent diameter	$[m]$	0.125	0.16
Young's Modulus	$[N/m^2]$	5.6e10	1.17e10
Unit weight in Air	$[N/m]$	1564.4	241.41
The ratio of weight in water to weight in air	$[kg/m]$	0.9218	0.16

The anchor position has been modified till the initial tension force reached 196.2 kN as designed. The positions of two ends for each line are listed in table 5.9.

Table 5.9: Fairlead and anchor position

Name	Attachment	Fairlead position [m]	Anchor position [m]
Line 1	Pontoon 2	[47.361, -27.5, -30]	[1017.7, -429.32, -150]
Line 2	Pontoon 2	[47.361, -27.5, -30]	[449.45, -997.57, -150]
Line 3	Pontoon 4	[-47.361, -27.5, -30]	[-449.45, -997.57, -150]
Line 4	Pontoon 4	[-47.361, -27.5, -30]	[-1017.7, -429.32, -150]
Line 5	Pontoon 6	[-47.361, 27.5, -30]	[-1017.7, 429.32, -150]
Line 6	Pontoon 6	[-47.361, 27.5, -30]	[-449.45, 997.57, -150]
Line 7	Pontoon 8	[47.361, 27.5, -30]	[449.45, 997.57, -150]
Line 8	Pontoon 8	[47.361, 27.5, -30]	[1017.7, 429.32, -150]

Mooring system in SIMA is shown in figure 5.7.
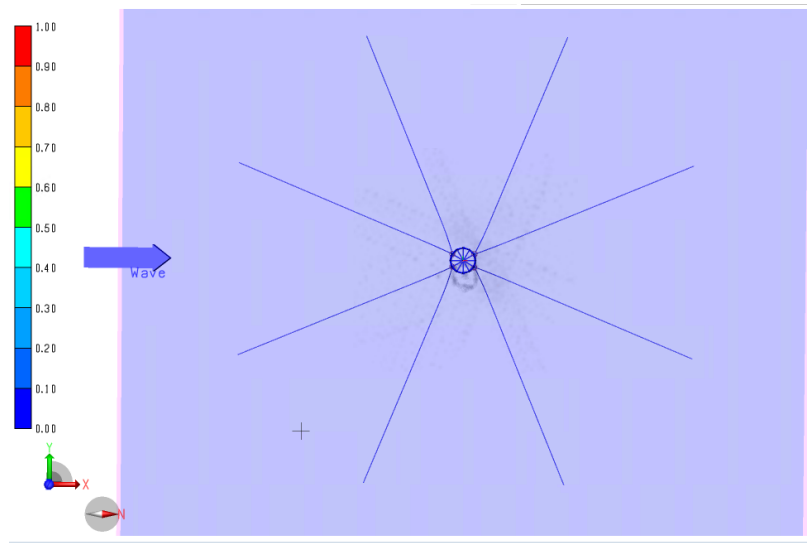
(a) Top view
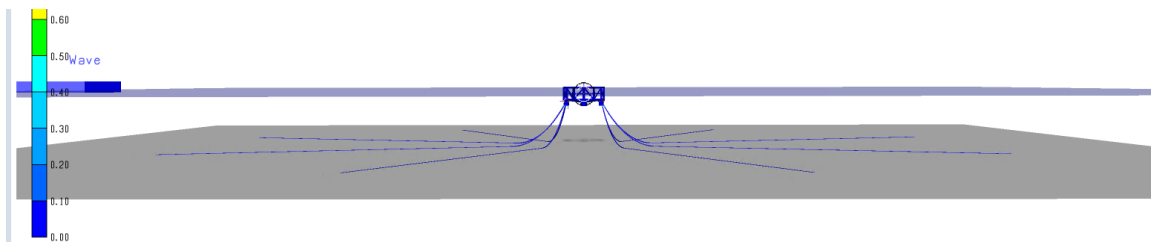
(b) Side view

Figure 5.7: Illustration of Mooring system in SIMA

5.3.3 Net Force Calculation

Instead of building net element, wave force on the net is added by calculation in an external file, which has instantaneously intercommunication with SIMA. In this section, the inter-communication method will be detailedly explained.

The external force calculation starts with reading input data from SIMA. The external communication rule of SIMA specifies that SIMA can output the following parameters in the communication[27]:

- Step number

- Time step and actual total time

- Density of water, density of air and gravity acceleration g

- Global position and velocity of the body

- current velocity in the environment condition

- Coordinate transformation matrix

Wave information is not transferred. Therefore, wave should be generated separately in the external file, which should has the same phase angle and time step as in SIMA model.

At each time step, SIMA will call the external function and export information mentioned above to it. Then wave force calculation will be made. Results including wave force components of 6 degrees of freedom will be transfered to SIMA.

The main steps of external wave force calculation are:

- Divide the net into smaller sub-panels and get the coordinates of panel centers

- Transfer the coordinates from local to global system and calculate wave information at these global points

- Derive the relative motion between wave and the structure

- Calculate wave force of each sub-net panel, sum all the force components and export to SIMA

Net Panel Division

The structure has 12 net panels on the side and 12 in the bottom. As it's in large dimension, net panels are divided into smaller sub-panels, as shown in figure 5.8.

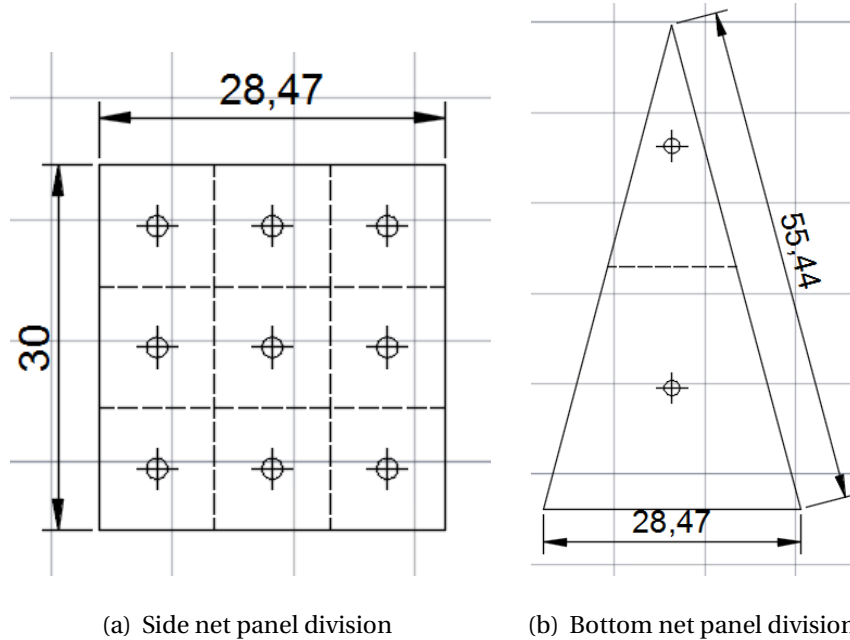| (a) Side net panel division | (b) Bottom net panel division |

Figure 5.8: Sub-panel division, dimension in meter

All the sub-panels on one side will have the same normal vector under local coordinate system. The area of each sub-panels are given in table 5.10

Table 5.10: Area of Sub-net panel

Sub-panels	Side sub-panel	Smaller sub-panel of bottom	Larger sub-panel of bottom
Area	$94.9 \ m^2$	$190.84 \ m^2$	$572.51 \ m^2$

Coordinate Transformation

Net panel vectors in local coordinate system are to be transferred to global coordinate system by transformation matrix, which is generated in SIMA. The transformation is mainly determined by 3 angles, ψ, θ and ϕ, where

- ψ is the body's rotation angle around the global z-axis

- θ is the body's rotation angle around the global y-axis

41

- ϕ is the body's rotation angle around the global x-axis

The matrix for coordinates transformation is:

$$\gamma = \begin{bmatrix} \cos\psi\cos\theta & -\sin\psi\cos\phi + \cos\psi\sin\theta\sin\phi & \sin\psi\sin\phi + \cos\psi\sin\theta\cos\phi \\ \sin\psi\cos\theta & \cos\psi\cos\phi + \sin\psi\sin\theta\sin\phi & -\cos\psi\sin\phi + \sin\psi\sin\theta\cos\phi \\ -\sin\theta & \cos\theta\sin\phi & \cos\theta\cos\phi \end{bmatrix} \quad (5.1)$$

For a vector represented by x^L in local system, the expression in global system is

$$x^G = \gamma \cdot x^L \quad (5.2)$$

When coordinates of position need to be transferred, the following theories should be applied:

Suppose the coordinates of body center in global system is (η_1, η_2, η_3) in the x-, y-, and z-direct5ions and angular displacements of the body in global x-, y- and z- axis is η_4, η_5, η_6. For a point in local coordinates system positioned at (x_L, y_L, z_L), the transformation to global system is:

$$x_G = \eta_1 + z\eta_5 - y\eta_6 \quad (5.3)$$

$$y_G = \eta_2 - z\eta_4 + x\eta_6 \quad (5.4)$$

$$z_G = \eta_3 + y\eta_4 - x\eta_5 \quad (5.5)$$

Force Calculation

When coordinates of each central point of sub-panels are transferred to global system, wave elevation and velocity at these position can be calculated. As lift force are at relative small values, only drag force are considered in the calculation.

At each time step, SIMA will generate new body motion information and transfer matrix. Coordinates and vectors in global coordinate system will be re-calculated. Drag coefficient, which relies on angle θ is a variable changing with motion and wave elevation. Drag force can be decided with known C_d.

Following are detail steps for drag force at time t for Sub-panel i:

- Central point coordinates in global coordinates system of sub-panel i is X_i: (x_i, y_i, z_i) and global normal vector is n_i. Area of sub-panel i is A_i

- Current velocity is U_c in x-axis direction and wave velocity at $X_i(x_i, y_i, z_i)$ is:

$$u_w = \omega \zeta_0 \cdot e^{kz_i} \sin(\omega - kx)$$

$$w_w = \omega \zeta_0 \cdot e^{kz_i} \cos(\omega - kx)$$

- Motion of the body from SIMA is (U_x, U_y, U_z), and relative motion $U_r(U_{x,r}, U_{y,r}, U_{z,r})$ is

$$U_{x,r} = u_w + U_c - U_x \tag{5.6}$$

$$U_{y,r} = 0 - U_y \tag{5.7}$$

$$U_{z,r} = w_w - U_z \tag{5.8}$$

- Angle between relative motion and normal vector of the panel is:

$$\cos\theta_i = \frac{U_r \cdot n_i}{|U_r| \cdot |n_i|} \tag{5.9}$$

- Drag coefficient at sub-panel i is :

$$C_{D,i} = 0.04 + (-0.04 + 0.33Sn + 6.54Sn^2 - 4.88Sn^3) \times |\cos\theta_i| \tag{5.10}$$

- Drag force of sub-panel i in relative motion direction is:

$$F_{D,i} = \frac{1}{2}\rho_{sw} \cdot C_{D,i} \cdot |U_r|^2 \cdot A_i \tag{5.11}$$

- Moment to the origin point due to the drag force is :

$$M_i = X_i \times F_{D,i} \tag{5.12}$$

Finally, force and moment are decomposed into x,y,z directions in global system and the 6-dof force components are summed to point (0,0,0), which will be transfer to SIMA.

5.4 Summary

Generally, the analysis process can be divided into 3 parts: geometry modeling in GeniE, hydrodynamic calculation in HydroD Wadam and time domain response analysis in SIMA, as shown in flowchart in figure 5.9.
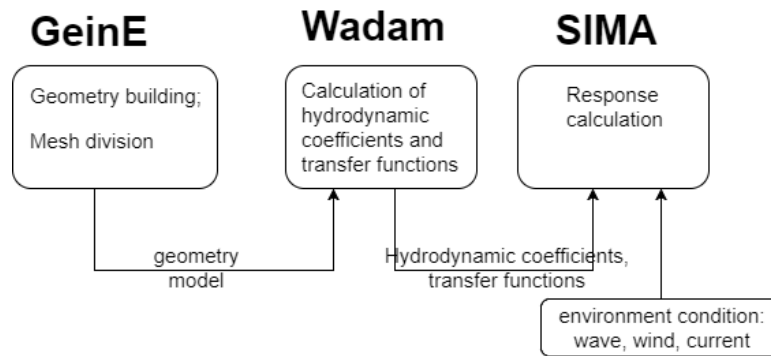
Figure 5.9: General analysis process
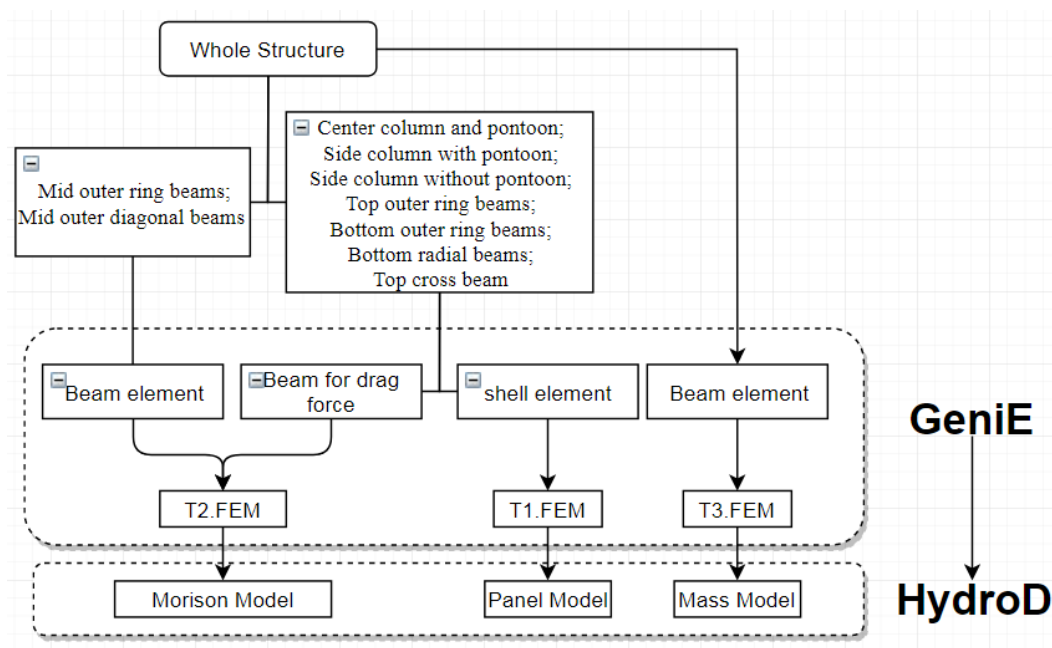
Figure 5.10: FEM modeling process

In this chapter, FEM modeling was firstly introduced. Three models have been built in Ge-niE, in which different structure components were included. The panel model, containing the main larger parts were modeled with shell elements, while both Morison model and mass

model built the structure with beam elements. FEM modeling in Genie and transfer to Hy-droD is illustrated in figure 5.10.

Hydrodynamic results from HydroD Wadam, including matrix and RAOs have been pre-sented. Natural frequencies were calculated and compared with experimental results.

The complete model in SIMA has been built, with all structural components and mooring systems included. Screen model application was covered and external force calculation method was proposed and explained detailedly. The general process of external force cal-culation is shown in figure 5.11.
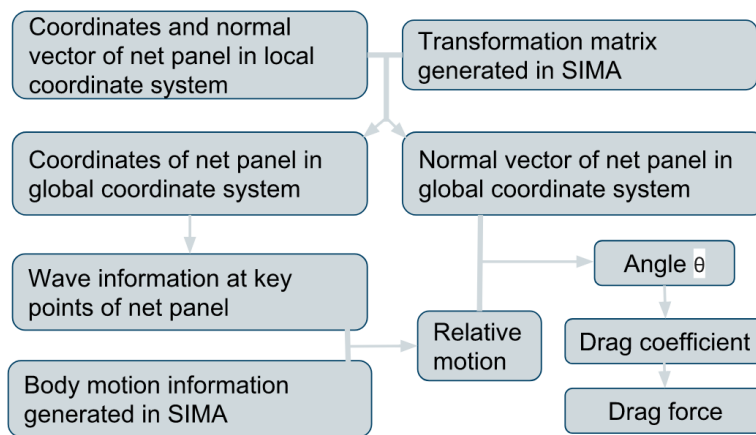
Figure 5.11: Calculation process for drag force on one sub-net panel

Chapter 6

Results and Comparison

In this chapter, time domain results in SIMA are shown and categorized by sea states into the following groups for a good comparison.

6.1   Validation under Steady Current Condition

Pål and Jørgen [11] have studied modified Morison method for calculating wave force on the net, in which they take Ocean Farm 1 as research object. They calculated the global performance of the modified Morison model by exposing the structure to a steady current of magnitude U_c = 0.75 m/s in 0 degree direction. They calculated the total in-line force on the net. Results are listed in table 6.1 compared with wave force calculated theoretically by Løland's screen model.

Table 6.1: Wave force results comparison

Modified Morison model[11]	Løland formula	Model in SIMA
742 [kN]	748 [kN]	740.6 [kN]

The same environment is applied and wave force on net calculated in SIMA is 740.6 kN, which is very close to Løland's theoretical results and Pål's study. The good agreement shows that both the structure modeling and force calculation method are satisfactory.

Wave force in other directions are also calculated and shown in figure 6.1. When current

comes in x-axis direction, drag force component in y-axis and z-axis direction are very small. Besides force in x-axis direction, moment to y-axis also plays an important role. In the case study of this thesis, Moment of y-axis is about -1.91 MNm.
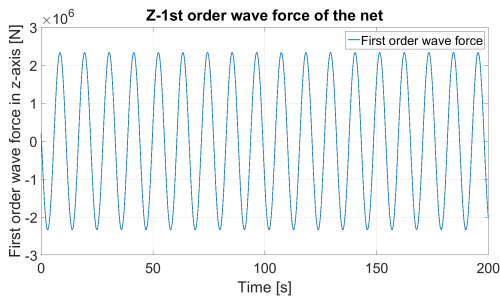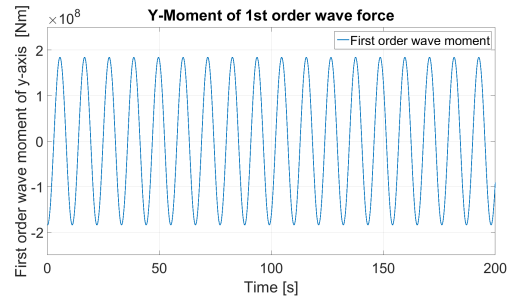

(a) X component
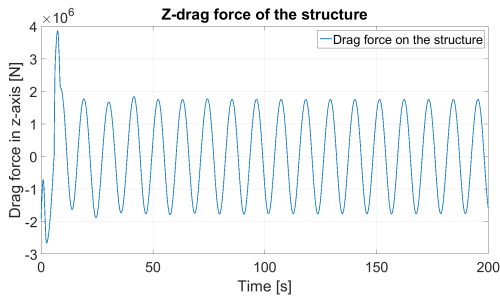
(b) Y component

(c) Z component

(d) Moment of Y-axis
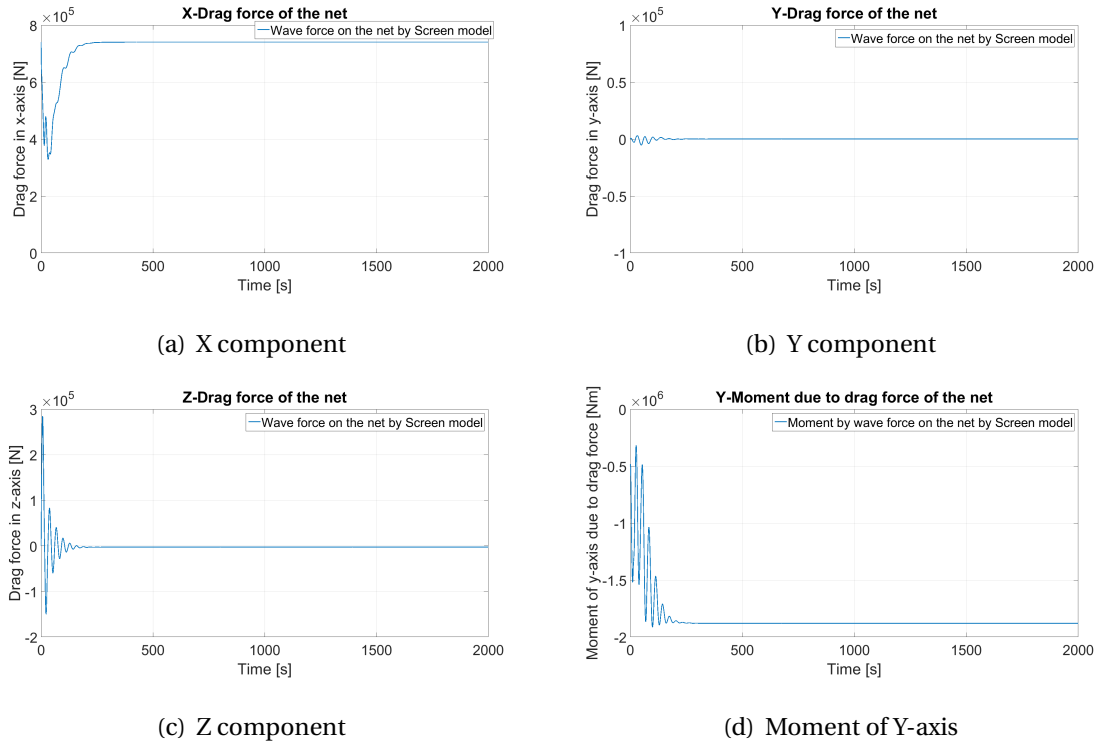
Figure 6.1: Drag force of cage net under only current in x-axis

6.2 Comparison between Force with and without Cage Net

6.2.1 Comparison between Wave Force on the Structure and Drag Force on the Net

To have a clear understanding of wave force proportions, first order wave force of the structure, drag force on the structure and drag force on the net have been calculated separately under the same wave condition of $H = 5$m and $T = 11$s.

The first order wave force and drag force of the structure under wave condition without net force into consideration are plotted in figure 6.2 and 6.3. Meanwhile, wave force on the net for the same structure and wave condition is also calculated by external file and plotted in figure 6.4. Force magnitude in steady states of the listed components are summarized in

table 6.2.
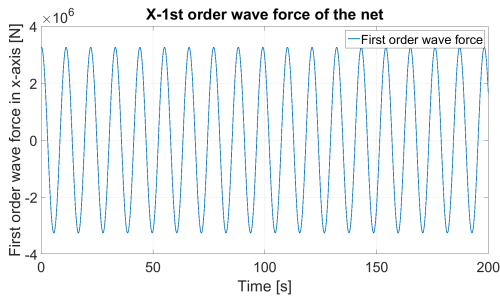
(a) X component
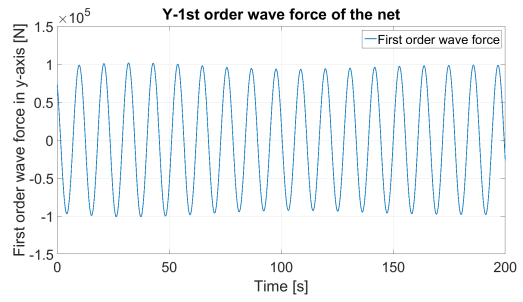
(b) Y component

(c) Z component

(d) Moment of Y-axis

Figure 6.2: First Order Wave Force under Wave $H = 5$m, $T = 11$s on the structure
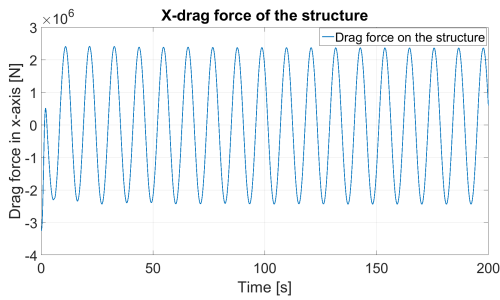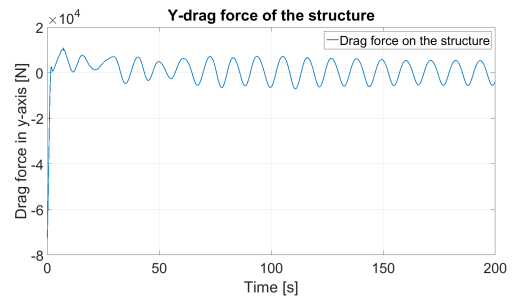
(a) X component

(b) Y component
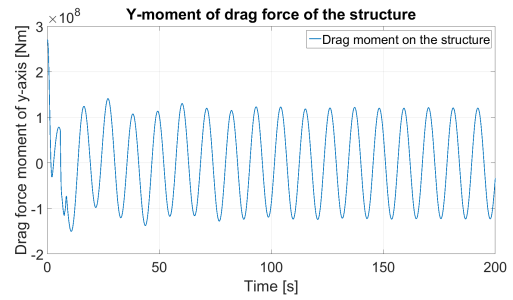
(c) Z component

(d) Moment of Y-axis

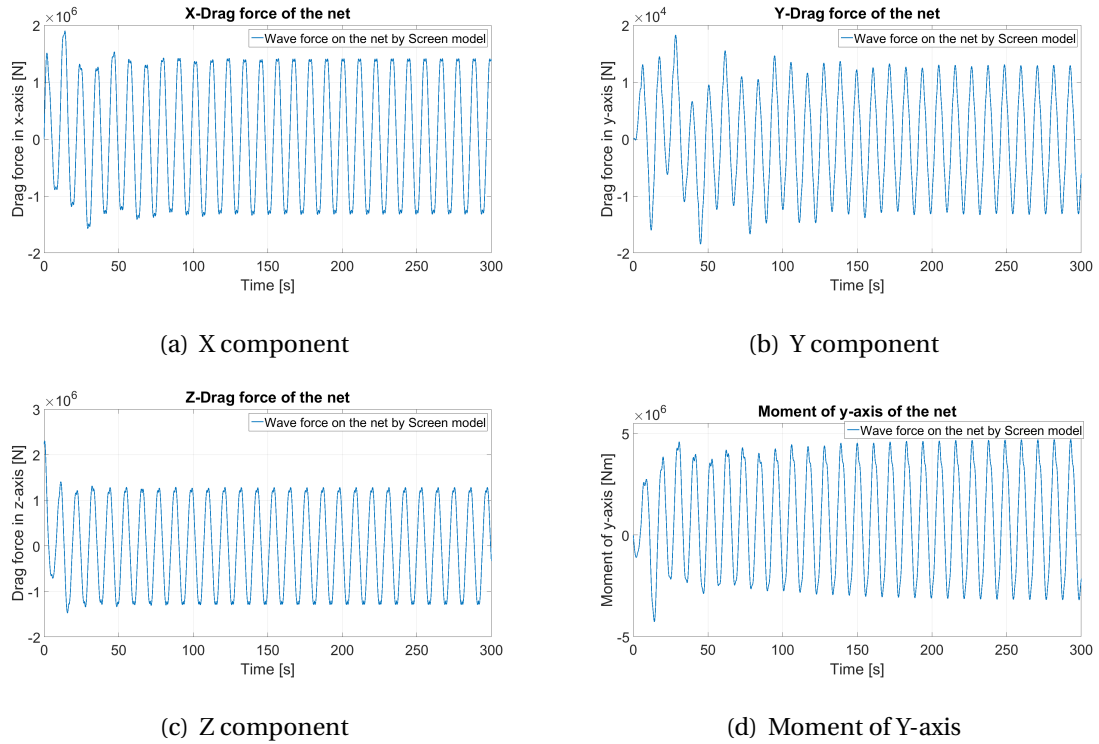Figure 6.3: Drag force under wave $H = 5$m, $T = 11$s on the structure

(a) X component

(b) Y component

(c) Z component

(d) Moment of Y-axis

Figure 6.4: Wave force on the net under wave $H = 5$m, $T = 11$s

Table 6.2: Comparison between Magnitude of Wave Force on the Structure and on the Net

Force Component	1st order force on the structure	F_d on the structure	F_d on the net
X-component	3.262 MM	2.37 MN	1.42 MN
Y-component	0.102 MN	0.005 MN	0.013 MN
Z-component	2.336 MN	1.77 MN	1.28 MN
Moment of y-axis	184.1 MNm	122.6 MNm	4.52 MNm

It can be seen that the dominating force components are in direction of x-axis, z-axis and moment of y-axis. First order wave force on the structure takes the largest proportion. For wave force in x- and z- direction, the three force components are different but at least in the same order. For moment of y-axis, drag force on the net counts for less than 1% of the total wave force moment.

As one of the emphasis of the thesis is net force calculation, the contribution of drag force on the net can be weighed from table 6.2. It takes about 15 % for the force in x- and z- direction. Therefore, net force cannot be disregarded.

6.2.2 Comparison of Mooring Line Force between Simulations with and without Cage Net

The system mooring line force by modeling with and without net force is compared, under wave state $H = 5$m, $T = 11$s. Total mooring force in 3-directions are plotted in figure 6.5 - 6.7. It can be seen that the effect of drag on total mooring force has is small in z and y-rotational direction. It mainly influences the x-component.
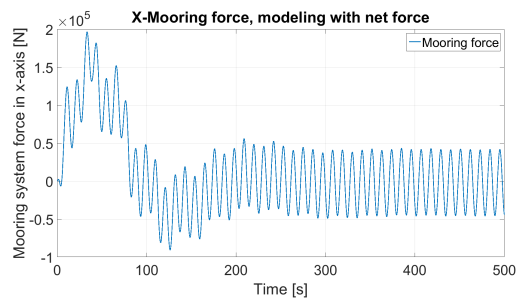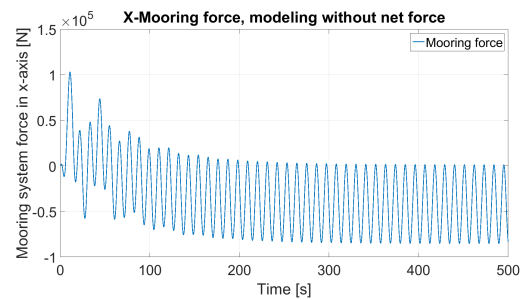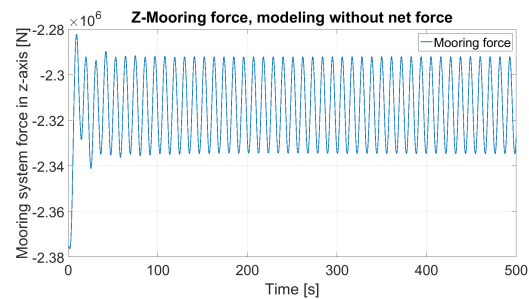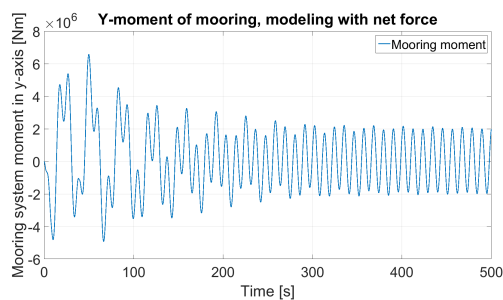

| (a) With net force | (b) Without net force |

Figure 6.5: Mooring force in x-direction, wave $H = 5$m, $T = 11$s
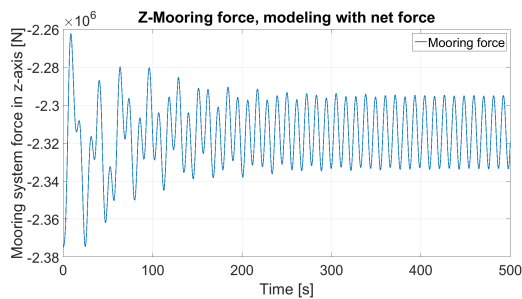
| (a) With net force | (b) Without net force |

Figure 6.6: Mooring force in z-direction, wave $H = 5$m, $T = 11$s
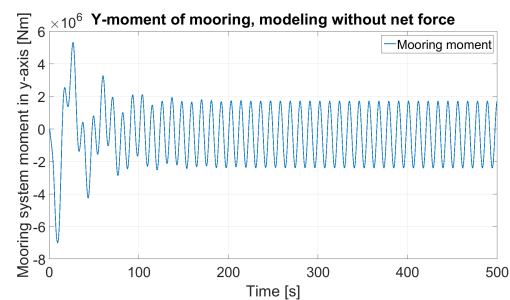
| (a) With net force | (b) Without net force |

Figure 6.7: Mooring force in y-rotation, wave $H = 5$m, $T = 11$s

6.2.3 Comparison of Motion Response between Simulations with and without Cage Net

The motion response would definitely be different when wave force on the net was considered or not. Sway, heave and pitch are the three motions to be focused when wave comes in 0 degree direction. Figure 6.8 and 6.9 shows the motion response results with wave condition $H = 5$m, $T = 11$s under simulations with and without cage net respectively. The magnitude of motion after the structure enters steady state are summarized in table 6.3.

Table 6.3: Comparison of motion response between modeling with and without wave force

Motion amplitude	Simulation without net force	Simulation with net force
Surge [m]	[0.341, -0.269]	[1.28, 0.316]
Sway [m]	[0.023, -0.007]	[0.023, -0.01]
Heave [m]	[-1.808, -2.865]	[-1.762, -2.961]
Pitch [deg]	[0.827, -0.842]	[0.937, -0.896]
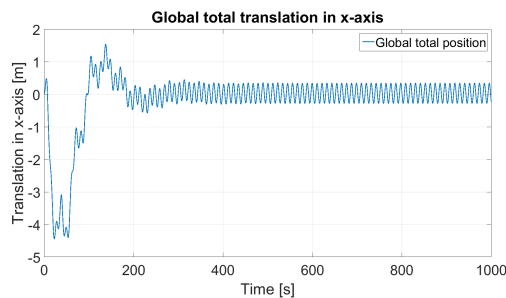
(a) Surge
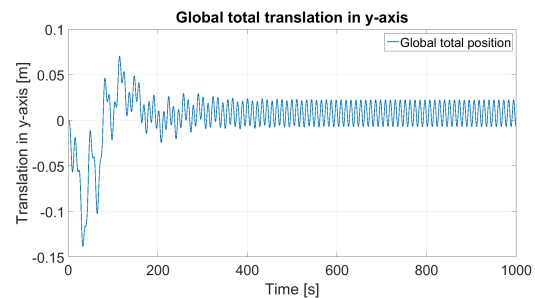
(b) Sway
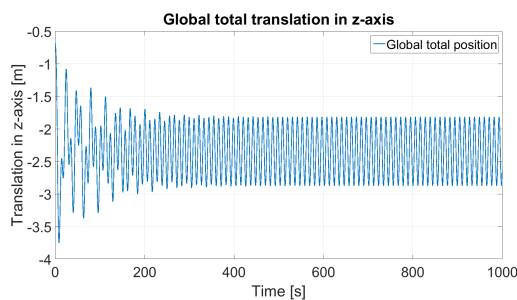
(c) Heave

(d) Pitch

Figure 6.8: Motion response under wave $H = 5$m, $T = 11$s without cage net
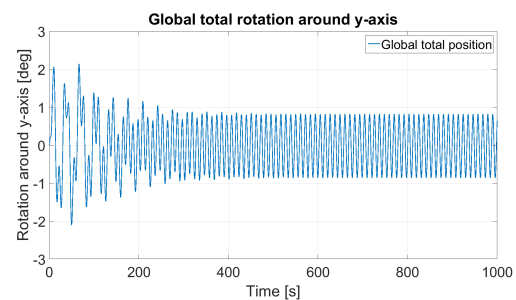
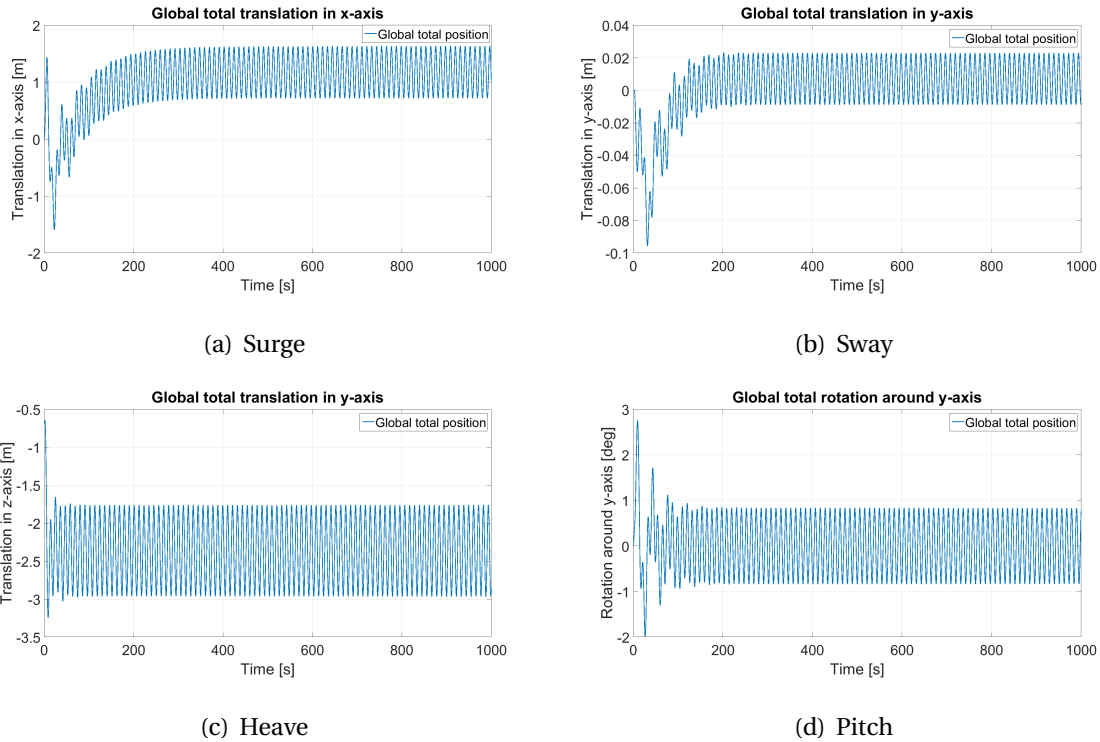(a) Surge

(b) Sway

(c) Heave

(d) Pitch

Figure 6.9: Motion response under wave $H = 5$m, $T = 11$s with cage net
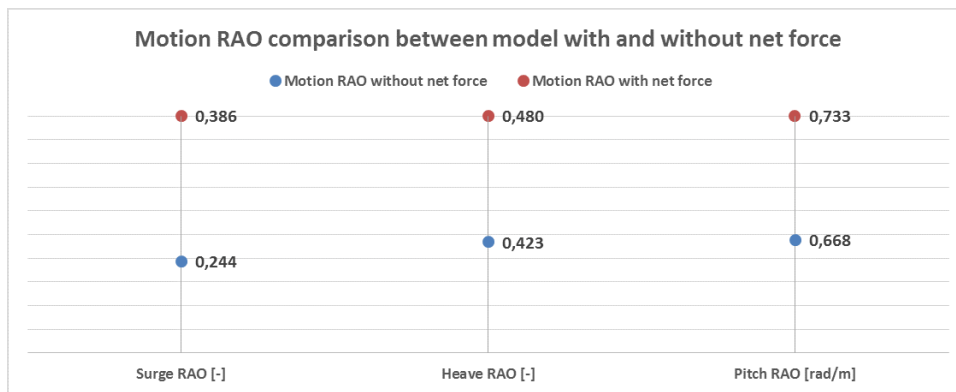

Figure 6.10: Comparison of motion RAO ($H = 5$m, $T = 11$s) between modeling with and without net force

It can be seen that surge, heave and pitch are motions with larger amplitude. With net force considered, the amplitude of motion would be improved. The mean position of surge moves towards the position direction of x-axis when net force is included. For heave and pitch, there's an increase on motion amplitude, while the mean positions are not much affected. Motion RAO is plotted in figure 6.10 for a clear illustration for the drag force on the net.

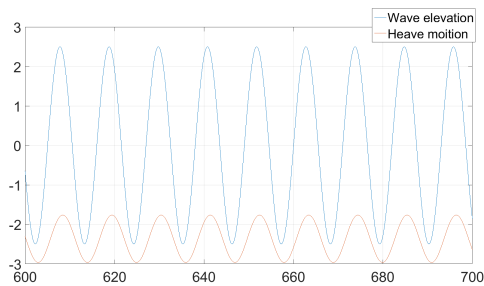## 6.2.4 Comparison of Phase Angle Shift between Simulations with and without Cage Net

Phase angle shifts between wave profile and motion profile are compared in this section.
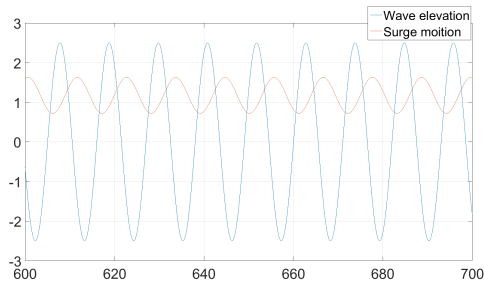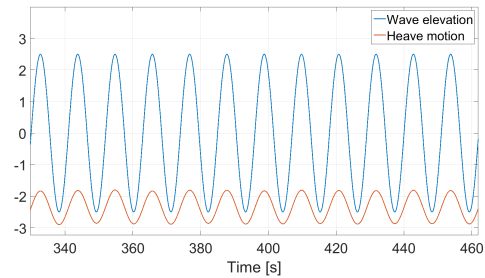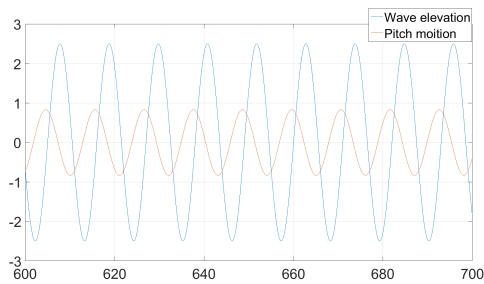

(a) Surge shift with net force
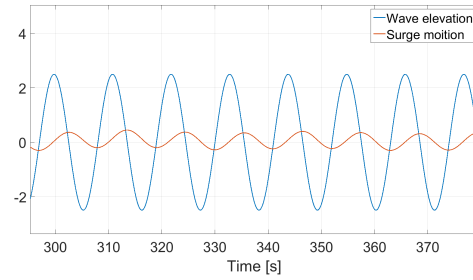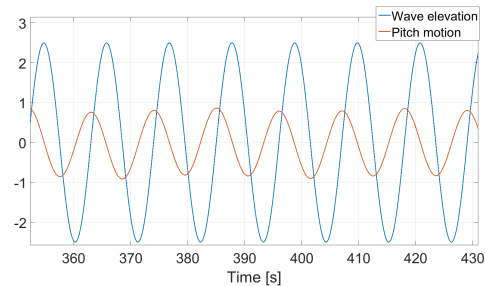
(b) Surge shift without net force

(c) Heave shift with net force

(d) Heave shift without net force

(e) Pitch shift with net force

(f) Pitch shift without net force

Figure 6.11: Phase shift in simulations with and without net force

As sway is not a dominating motion under the studied wave states, only surge, heave and pitch are considered in this section and all following chapters. Figure 6.11 and table 6.4 show the shift angle resulted in simulations with and without net force.

54

Table 6.4: Comparison of motion response between modeling with and without wave force

Phase shift	Simulation without net force	Simulation with net force
Surge [rad]	$\pi/2$	$2\pi/3$
Heave [rad]	0	$\pi/6$
Pitch [rad]	$-\pi/2$	$-\pi/3$

We can see that surge motion is $\pi/2$ ahead to wave, while pitch is $\pi/2$ lagging behind when net force is not considered. Heave motion has the same phase with wave elevation. Drag force on the net can bring a $\pi/6$ phase shift.

6.3   Comparison among Regular Wave States

In this section, 12 regular waves are chosen as studied sea states, as listed in table 6.5.

Table 6.5: Wave states

NO.	H [m]	T [s]	NO.	H [m]	T [s]
1		5	7		5
2		7	8		7
3	1	9	9	5	9
4		11	11		11
5		13	12		13
6		15	13		15

6.3.1   Wave Force Comparison

The components in three directions of drag force on the net, 1st order wave force on the structure and total wave force are plotted respectively under the 12 wave conditions.

X-Force

Figure 6.12 shows x-component of 1st order wave force on the structure. It illustrated that larger wave height leads to a higher force amplitude. When wave period is longer than 9 seconds, force amplitude will also increase with wave period. The transition at 9 second can be explained by the wave force cancellation effect.
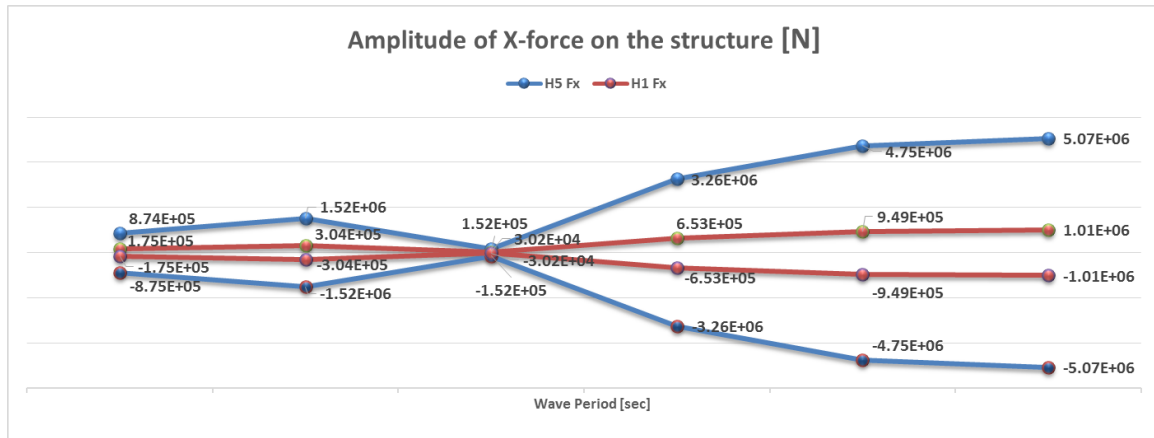

Figure 6.12: X-component of 1st order wave force on the structure

Wave force cancellation would happen when the main dimension of the structure is close to wave length, as the two end of the structure will be at wave crest and trough, respectively, which leads to wave force in same magnitude but opposite directions. Thus the total acting force on the structure will be quite small.

The diameter of Ocean Farm 1 is 110 m, for which wave force cancellation would happen when wave length is at close value, and the corresponding wave period is

$$T = \sqrt{2\lambda \cdot \pi / g} = 8.4 \quad \text{sec} \tag{6.1}$$

9 second wave period is very close to the force cancellation range. Therefore there is a falling at 9 second.

Figure 6.13 compares the amplitude of x-component of drag force on the net under 12 wave conditions. Contrarily, drag force has a trend to decrease with increasing wave period.

Figure 6.14 gives the comparison of total wave force on the whole structure. The amplitude is not a simple superposition of maximum drag force and 1st order wave force, as the two

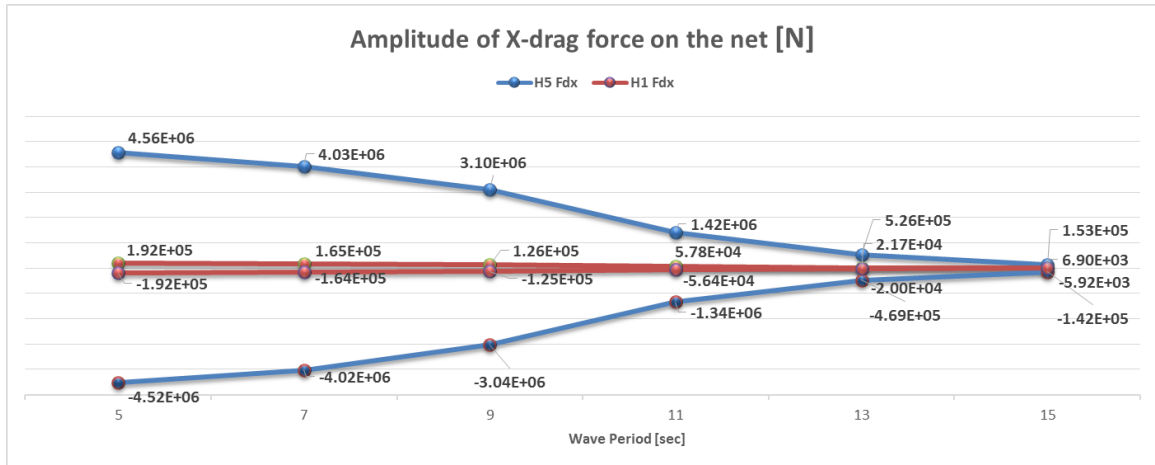force has an phase shift.

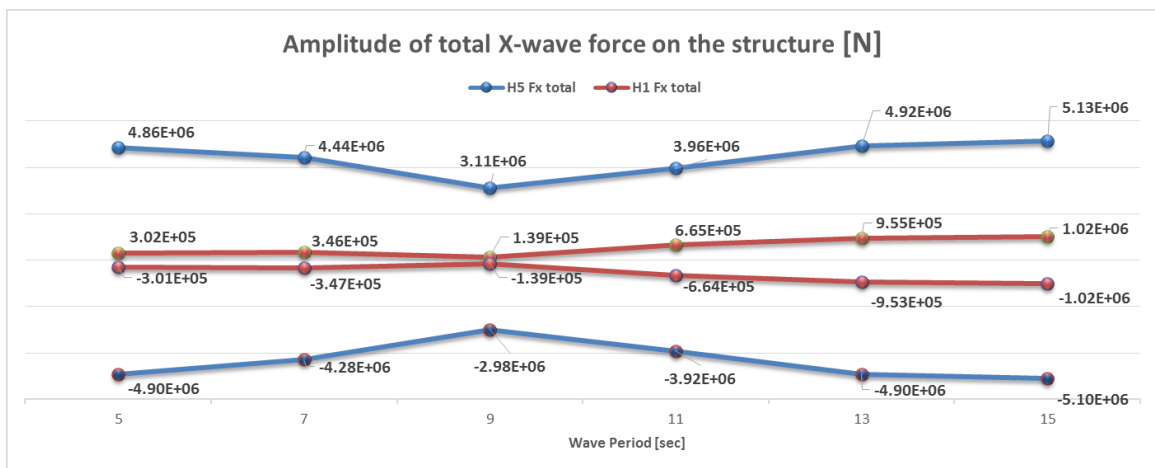Figure 6.13: X-component of drag force on the net

Figure 6.14: X-component of total wave force on the structure

It can be concluded that the total force could be affected by wave height. Wave with larger amplitude will have higher velocity, which is the main consideration for wave force. For Wave period, it mainly affects the force cancellation level.

Z-Force

Heave motion of the structure largely depends on wave force component in z-axis.

Figure 6.15 shows 1st order wave force on the structure. Similar to X-force component, wave force in z-direction also includes with increasing wave period. The influence of wave ampli-

tude is small with shorter wave period. When wave period is longer than 9 seconds, wave height has a stronger effect in improving wave force in z-axis direction.

Figure 6.16 shows the relation between drag force on the net and wave condition. Large wave height would generate a height amplitude of drag force in z-direction, while large wave period would decrease drag force.

Figure 6.17 compares the total wave force in z-direction on the structure. When weight height is 5 m, the total wave force in z-direction would slight decrease with longer wave period, while for 1-m-wave height, there is a opposite trend.
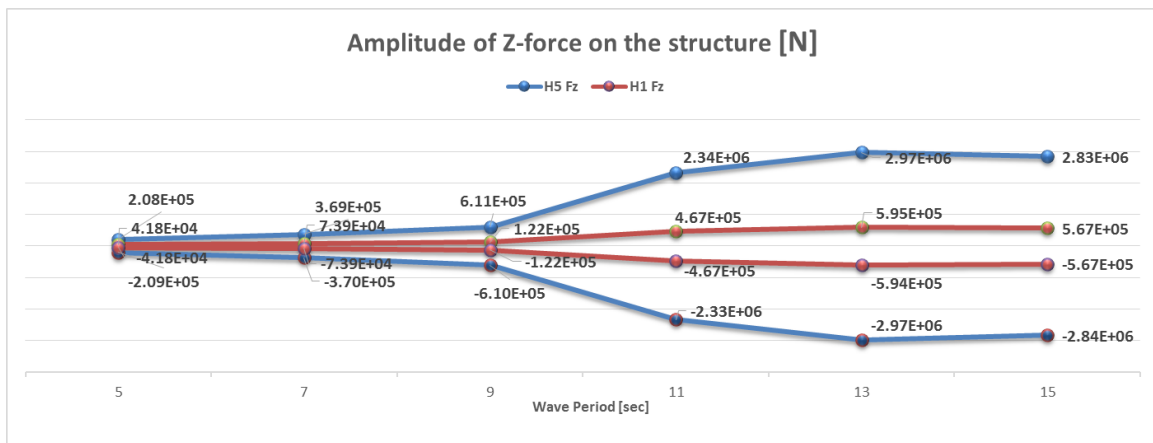

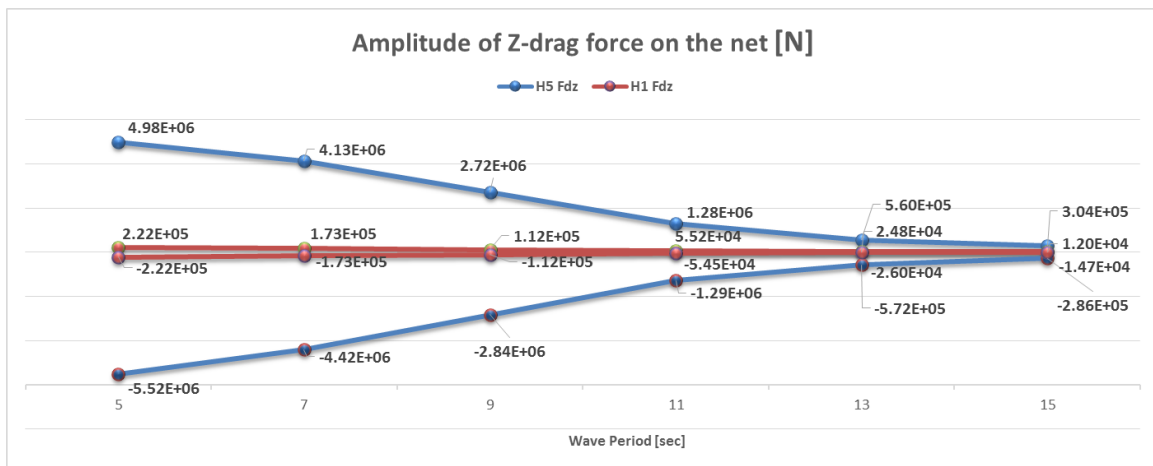Figure 6.15: Z-component of 1st order wave force on the structure
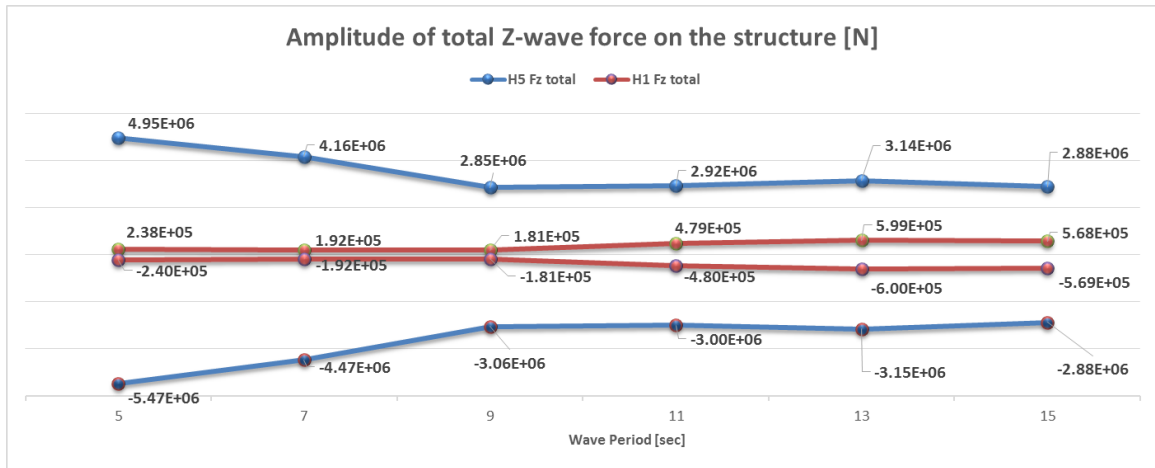

Figure 6.16: Z-component of drag force on the net

Figure 6.17: Z-component of total wave force on the structure

Moment of Y-axis

Moment of y-axis is the vital force component that determines pitch motion.

Figure 6.18 shows that pitch moment as 1st order wave force on the structure would increase with with longer wave periods, while in figure 6.19, pitch moment caused by cage net would decrease with improving wave period. When considering the total pitch moment, as shown in figure 6.20, it keeps the same trend as the 1st order pitch moment acting on the structure.

This indicates that the pitch moment is mainly determines by 1st order wave force. The pitch moment acting on the structure takes a larger percentage than that acting on the net.
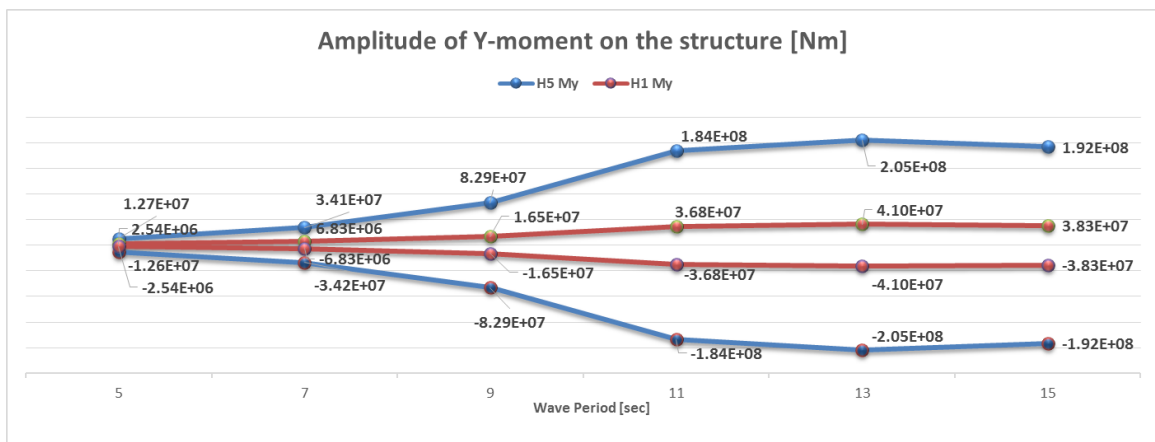

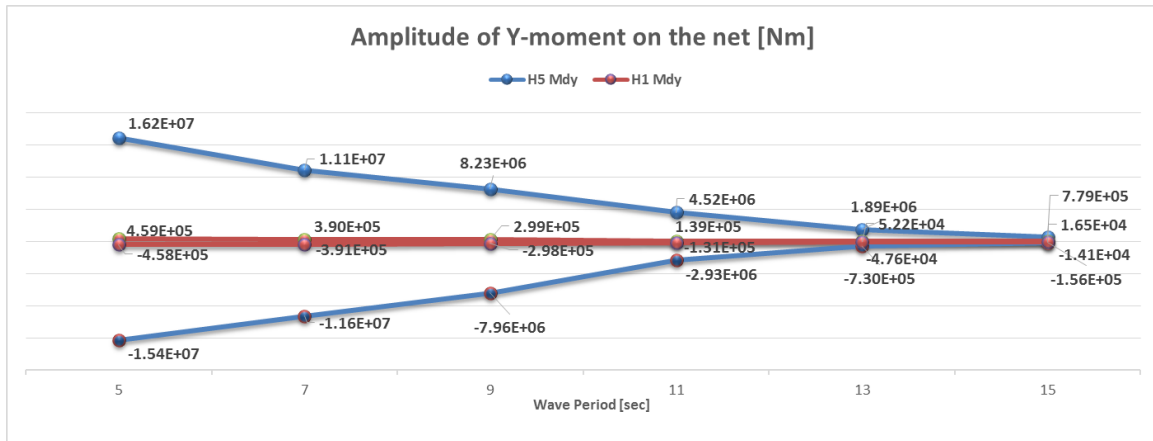Figure 6.18: Moment of y-axis of 1st order wave force on the structure

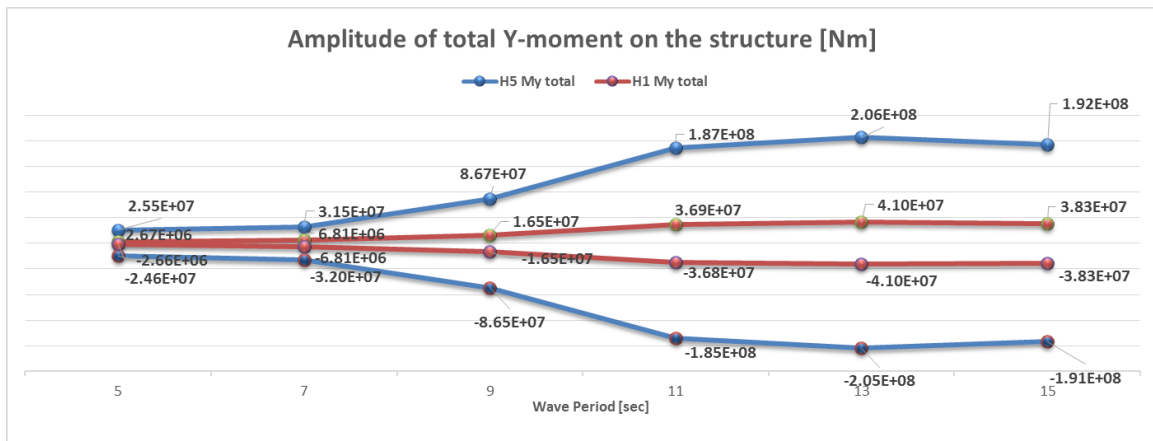Figure 6.19: Moment of y-axis of drag force on the net

Figure 6.20: Moment of y-axis of total wave force on the structure

### 6.3.2   RAO and Phase Shift Comparison

RAO of wave loads

Wave loads are then evaluated as RAO functions as shown in figure 6.21-6.23.

For wave loads in x and z-directions, 1st order force is the leading force component when H is 1m. Drag force on the net is of small account. When wave height increase to 5m, drag force shows its effect, especially at shorter periods. This is because drag force is of second order to wave velocity, which largely depends on wave frequency. As wave period increase, wave frequency becomes lower, which leading to smaller drag force.
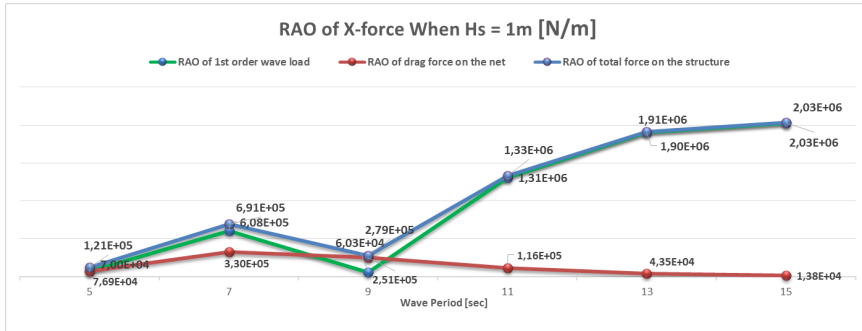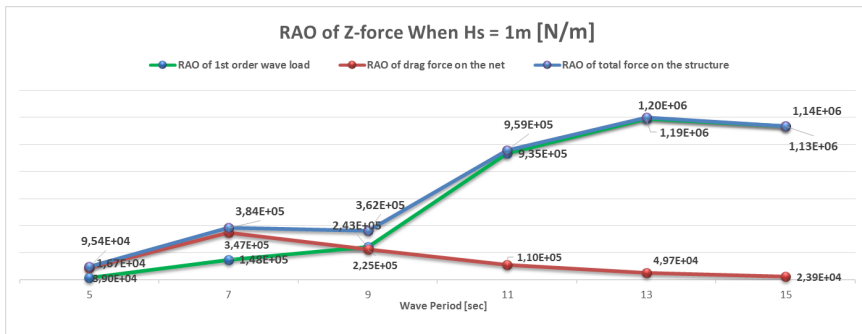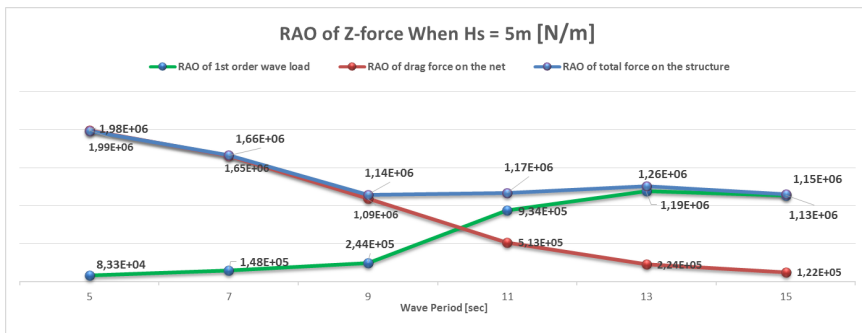
(a) Fx RAO when $H = 1$m
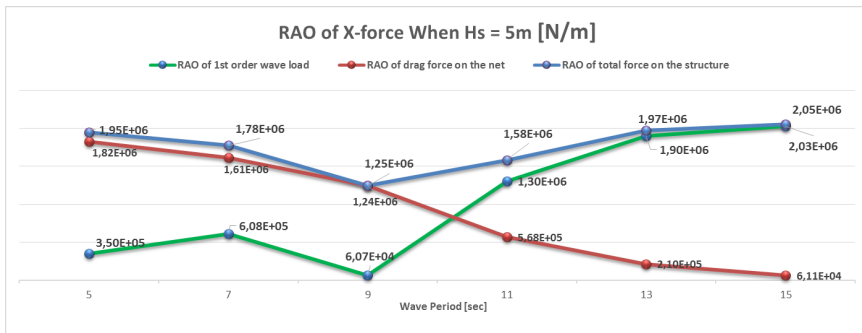
(b) Fx RAO when $H = 5$m

Figure 6.21: RAO of Fx for wave height 1m and 5m

(a) Fz RAO when $H = 1$m

(b) Fz RAO when $H = 5$m

Figure 6.22: RAO of Fz for wave height 1m and 5m
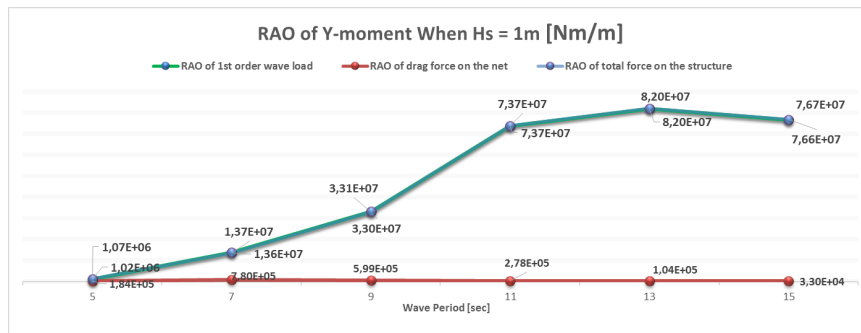
(a) My RAO when $H = 1$m
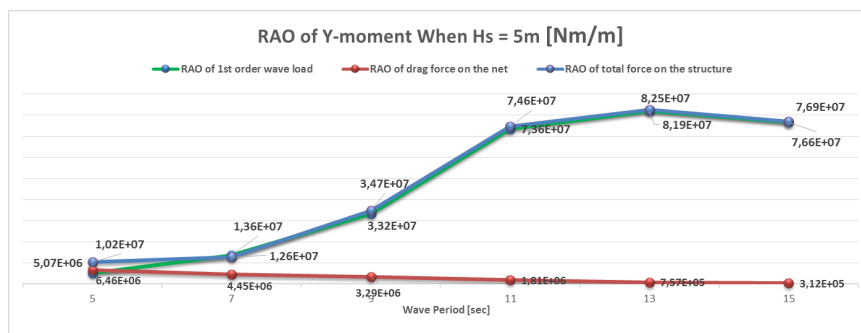
(b) My RAO when $H = 5$m

Figure 6.23: RAO of My for wave height 1m and 5m

When it comes to moment component of wave loads, the same conclusion can be achieved for both wave height. Drag force on the net only accounts for about 1% of total net force. The trend of total pitch force almost keep same with first order pitch force.

RAO of surge, heave and pitch have been calculated and illustrated in figure 6.24 - 6.26.

Figure 6.24: RAO of surge motion
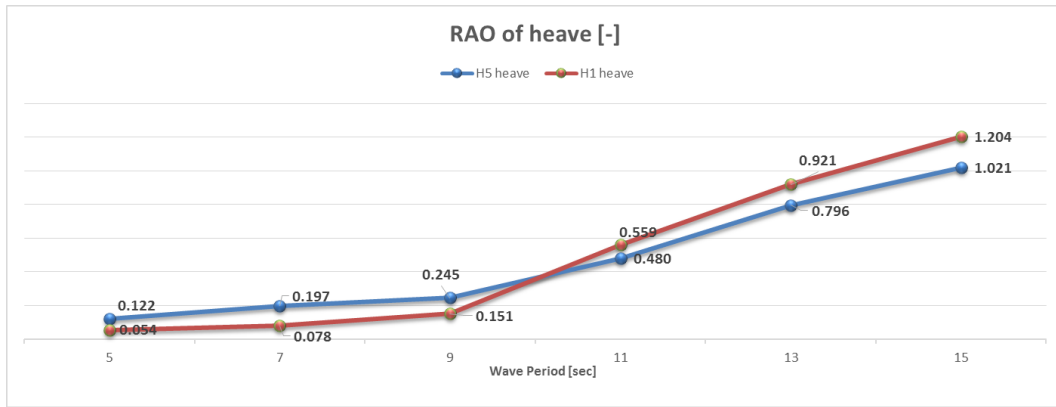
Figure 6.25: RAO of heave motion
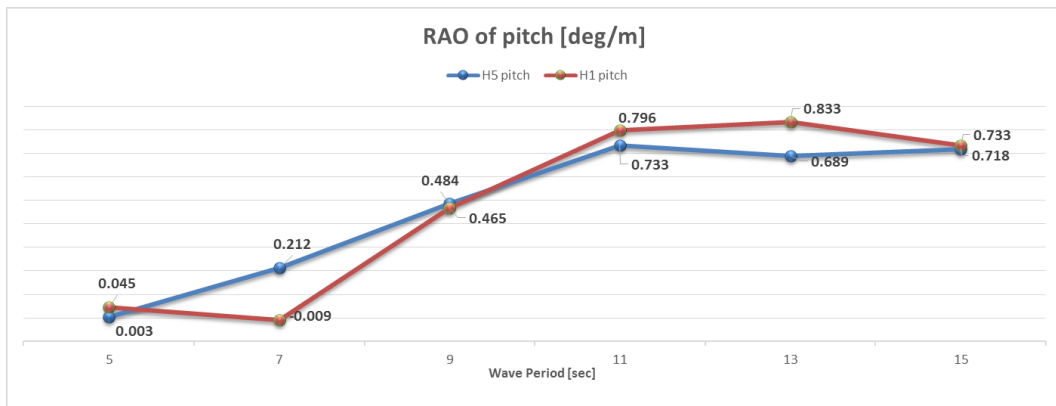
Figure 6.26: RAO of pitch motion

It shows that RAO for all three motions will increase for both two wave height, when raising wave period. The increasing trends differs with motions. For translation motions, i.e., surge and heave, there's a slow increase in shorter wave periods, but a 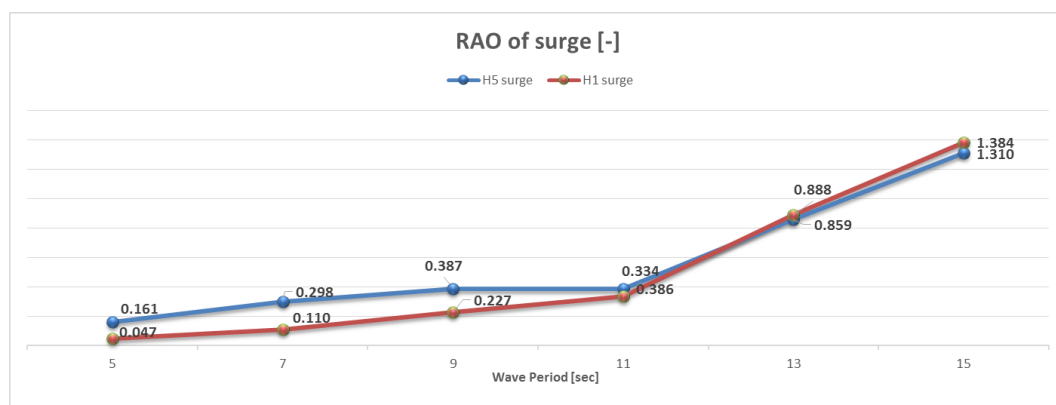higher improvement in long wave periods. While for rotation motion like pitch, the conclusion is opposite. Intensive increase happens in lower wave period. When Tp is larger than 11s, there's almost no increasing tendency.

The effect of wave amplitude varies with wave period. In shorter wave period (Tp<10s), a larger wave amplitude leads to a higher RAO than smaller wave amplitude, while when Tp>10s, 1-meter-high wave will surpass 5-meter-high wave and gives a higher RAO.

RAO can only reflect the amplitude relation between wave and motion. There is also a phase shift between wave and motion profile. For different motions and wave states, the shift angle varies as listed in table 6.6 and figure 6.27 -6.29.

Table 6.6: Phase shift between motion and wave profile [rad]

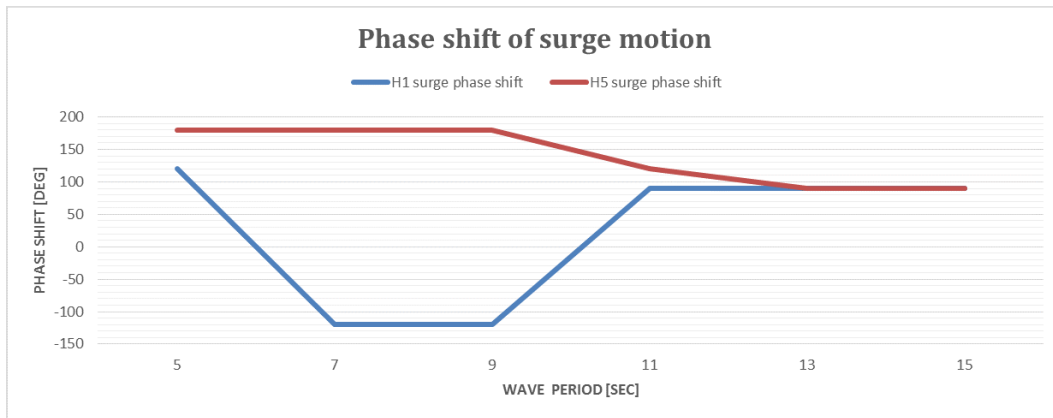| Motion	H1T5	H1T7	H1T9	H1T11	H1T13	H1T15
Surge	$\frac{2}{3}\pi$	$-\frac{2}{3}\pi$	$-\frac{2}{3}\pi$	$\frac{1}{2}\pi$	$\frac{1}{2}\pi$	$\frac{1}{2}\pi$
Heave	$\frac{1}{2}\pi$	$\frac{2}{3}\pi$	$\frac{1}{3}\pi$	0	0	0
Pitch	$\frac{2}{3}\pi$	π	$-\frac{1}{2}\pi$	$-\frac{1}{2}\pi$	$-\frac{1}{2}\pi$	$-\frac{1}{2}\pi$
	H5T5	H5T7	H5T9	H5T11	H5T13	H5T15
Surge	π	π	π	$\frac{2}{3}\pi$	$\frac{1}{2}\pi$	$\frac{1}{2}\pi$
Heave	$\frac{1}{2}\pi$	$\frac{1}{2}\pi$	$\frac{1}{3}\pi$	$\frac{1}{6}\pi$	0	0
Pitch	$-\frac{2}{3}\pi$	π	$-\frac{1}{3}\pi$	$-\frac{1}{2}\pi$	$-\frac{1}{2}\pi$	$-\frac{1}{2}\pi$

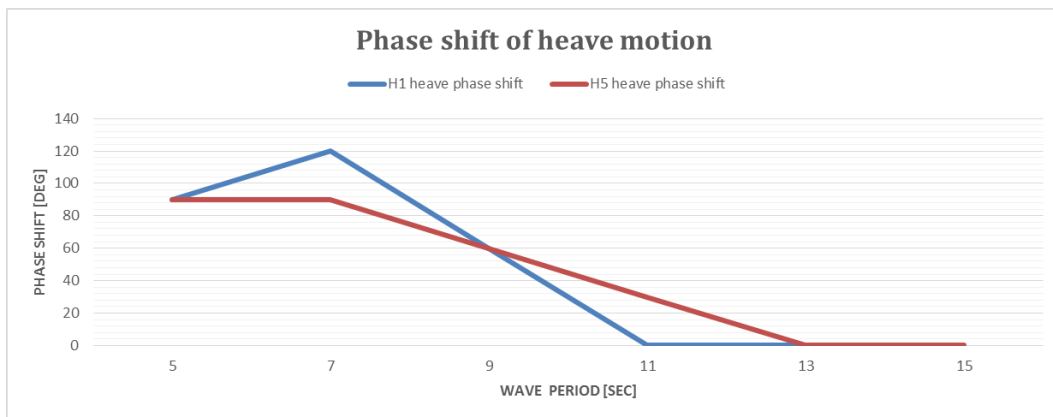
Figure 6.27: Phase shift of surge motion

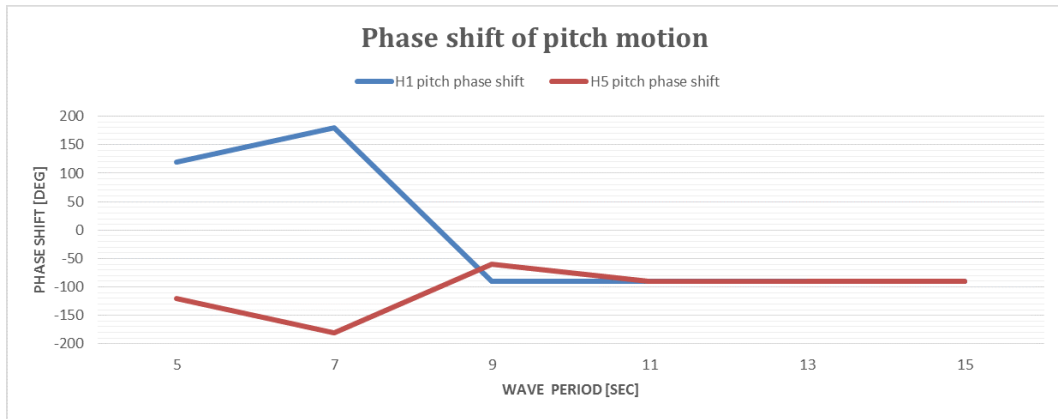Figure 6.28: Phase shift of heave motion

Figure 6.29: Phase shift of pitch motion

Chapter 7

Summary and Future Works

7.1 Summary

The main achievements in this thesis are listed as follows:

- A complete FEM model, including panel model, mass model and Morison model has been built.

- Hydrodynamic properties in frequency domain have been calculated.

- Mooring system was built as part of the model

- Screen model was applied and an external communicative file was programmed for the calculation of wave force on the net.

- Response of the structure under 13 sea states were studied and compared.

Regarding the calculation, results have been presented in chapter 6. A summary of discussion is given in this section.

- The steady current state was first calculated and the results shows a good agreement with previous research. Therefore, the modeling is seen accurate and calculation method is applicable.

- Two models, with and without cage net were then compared under a certain wave state to find the scale of net force. Drag force on the net can be concluded to be at a small level than wave force on the structure. The influence on motion amplitude is not large,

but effect on mean position of the body and phase shift of the motion cannot be neglected. Therefore, wave force on the net should be considered for response analysis.

- Modeling with net force under 12 wave states are finally studied for a comparison of force and motion. Both wave height and wave period will affect the acting force and transfer function and the effect of wave height is more predictable. It should be pointed that the wave periods studied in this thesis, which is also the representative sea state at the operating site, Frohavet sea, are far from the natural period of the structure, as listed in table 5.6. Therefore, the structure is working in a relative safe condition.

7.2   Future Work

The study accomplished in this master thesis mainly focused on the numerically modeling and motion response analysis of Ocean Farm 1 concept. There is a wide scope for further researches regarding this semi-submersible fish cage concept. Below is a list of suggestions for improvement and future studies:

- Structure modeling In this thesis, the mass model is a simplification with mass point to get the correct gravity center position. A better mass model with more precise mass distribution can be built for a more correct mass matrix in hydrodynamic analysis.

- Environment condition

  Several regular wave states and steady current are studied in this thesis work. For more practical analysis, wind load and irregular waves can be applied.

- Stress analysis

  By build the structure as one rigid body model, the motion response has been calculated in this thesis. To estimate the life expectation and evaluate safety reliability, stress calculation and fatigue analysis can be made by build the structure as a flexible model.

Bibliography

[1] http://www.fao.org/fishery/facp/NOR/en.

[2] http://www.fao.org/figis/common/format/popUpImage.jsp?xp_imageid=35604.

[3] http://web.msicom.net/wordpress/productos/plataforma-offshore/?lang=en.

[4] http://www.sadco-shelf.com/?d[]=products.

[5] http://www.refamed.com/gabbie_mare/tlc_system.html.

[6] https://www.salmar.no/en/offshore-fish-farming-a-new-era/.

[7] https://subseaworldnews.com/2017/04/04/lankhorst-to-deliver-mooring-lines-for-salmars-aquaculture-project/.

[8] https://www.sintef.no/en/projects/offshore-salmon-fish-farming/.

[9] https://subseaworldnews.com/2017/04/04/lankhorst-to-deliver-mooring-lines-for-salmars-aquaculture-project/.

[10] http://www.akvagroup.com/products/cage-farming-aquaculture/nets/econet.

[11] PÅL T. BORE, JØRGEN AMDAHL, and DAVID KRISTIANSEN. "MODELLING OF HYDRODYNAMIC LOADS ON AQUACULTURE NET CAGES BY A MODIFIED MORISON MODEL". In: *VII International Conference on Computational Methods in Marine Engineering* (2017).

[12] Bernt Ege and Karl Strømsem. *Transferring oil,gas technologies to aquaculture*. Tech. rep. 2016.

[13] Chai-Cheng Huang, Hung-Jie Tang, and Jin-Yuan Liu. "Dynamical analysis of net cage structures for marine aquaculture: Numerical simulation and model testing". In: *Aquacultural Engineering* 35 (2006), pp. 258–270.

[14] Østen Jensen, Anders Sunde Wroldsen, and Pål Furset Lader. "Finite element analysis of tensegrity structures in offshore aquaculture installations". In: *aquaculture engineering* 36 (2007), pp. 272–284.

[15] Pascal Klebert, Pål Lader, and Lars Gansel. "Hydrodynamic interactions on net panel and aquaculture fish cage: A review". In: *Ocean Engineering* 58 (2013), pp. 260–274.

[16] Trygve Kristiansen and Odd M. Faltinsen. "Modelling of current loads on aquaculture net cages". In: *Journal of Fluids and Structures* 34 (2012), pp. 218–235.

[17] Lin Li and YMuk Chen Ong. "A PRELIMINARY STUDY OF A RIGID SEMI-SUBMERSIBLE FISH FARM FOR OPEN SEAS". In: *36th International Conference on Ocean, Offshore and Arctic Engineering* (2017).

[18] Geir Loland. "Current forces on, and water flow through and around, floating fish farms". In: *Aquaculture International* (1993), pp. 72–89.

[19] *Ministry of Fisheries and Coastal Affairs*. Tech. rep. 2011.

[20] Heidi Moe-Føre, Per Christian Endresen, and Karl Gunnar Aarsæther. "Structural Analysis of Aquaculture Nets: Comparison and Validation of Different Numerical Modeling Approaches". In: *Journal of Offshore Mechanics and Arctic Engineering* 137 (2015), pp. 041201-1–041201-7.

[21] *Offshore Fish Farming - A new era*. Tech. rep.

[22] O.M.Faltinsen. *Sea Loads on Ships and Offshore Structure*. Cambridge University Press, 1990.

[23] Pål.T.Bore and Pål.A.Fossan. *Ultimate-and Fatigue Limit State Analysis of a Rigid Offshore Aquaculture Structure*. 2015.

[24] *RECOMMENDED PRACTICEDET NORSKE VERITASDNV-RP-C205, ENVIRONMENTAL CONDITIONS AND ENVIRONMENTAL LOADS*. DNV, 2010.

[25] *SIMO 4.8.4 Theory Manual*. MARINTEK, 2016.

[26] *SIMO 4.8.4 User Guide*. MARINTEK, 2016.

[27] *SIMO-User's MAnual*. Tech. rep. 2009.

[28] Igor Tsukrov, Oleg Eroshkin, and David Fredriksson. "Finite element modeling of net panels using a consistent net element". In: *Ocean Engineering* 340 (2003), pp. 251–0270.

[29] Yun-Peng Zhao et al. "A numerical study on dynamic properties of the gravity cage in combined wave-current flow". In: *Ocean Engineering* 34 (2007), pp. 2350–2363.

Appendix A

SIMO Introduction

SIMO is a simulation program, which can calculate the motion behavior of floating vessels and structures. It has the following essential features [26]:

- Flexible modeling on multi-body system;

- Nonlinear time-domain simulation of wave frequency as well as low frequency forces;

- Environmental forces due to wind, waves and current;

- Passive and active control force;

- Interactive or batch simulation.

It mainly consists of five models as shown in figure A.1.

SIMO	INPMOD	File system for communication between modules	Input generation and presentation, interface to external sources of data
	STAMOD		Read input data, static analyses, define initial condition
	DYNMOD		Dynamic analyses, generation of time series
	OUTMOD		Post-processing of time series
	S2XMOD		Export of time series

Figure A.1: Modules of SIMO [25]

Appendix B

Supplementary Data of Results

In this chapter, numbers regarding net panel are listed. Table B.1 shows the normal vector of net panels in initial local coordinate system. Table B.2 gives the coordinates of center point of each sub panel on the bottom.

Table B.1: Normal vector of net panels

Panel number	Bottom panel normal vector	Side panel normal vector
1	(0.16, -0.04, -0.99)	(0.97, -0.26, 0.00)
2	(0.12, -0.12, -0.99)	(0.71, -0.71, 0.00)
3	(0.04, -0.16, -0.99)	(0.26, -0.97, 0.00)
4	(0.04, 0.16, 0.99)	(0.26, 0.97, 0.00)
5	(0.12, 0.12, 0.99)	(0.71, 0.71, 0.00)
6	(0.16, 0.04, 0.99)	(0.97, 0.26, 0.00)
7	(0.16, -0.04, 0.99)	(0.97, -0.26, 0.00)
8	(0.12, -0.12,0.99)	(0.71, -0.71, 0.00)
9	(0.04, -0.16, 0.99)	(0.26, -0.97, 0.00)
10	(0.04, 0.16, -0.99)	(0.26, 0.97, 0.00)
11	(0.12, 0.12, -0.99)	(0.71, 0.71, 0.00)
12	(0.16, 0.04, -0.99)	(0.97, 0.26, 0.00)

Table B.2: Coordinates of central point of bottom sub-panel in initial local system

| Panel	Subpanel	x	y	z
Pane l1	sub1	13.28	-3.56	-33.75
	sub2	39.84	-10.68	-29.25
Panel 2	sub1	9.72	-9.72	-33.75
	sub2	29.17	-29.17	-29.25
Panel 3	sub1	3.56	-13.28	-33.75
	sub2	10.68	-39.84	-29.25
Panel 4	sub1	-3.56	-13.28	-33.75
	sub2	-10.68	-39.84	-29.25
Panel 5	sub1	-9.72	-9.72	-33.75
	sub2	-29.17	-29.17	-29.25
Panel 6	sub1	-13.28	-3.56	-33.75
	sub2	-39.84	-10.68	-29.25
Panel 7	sub1	-13.28	3.56	-33.75
	sub2	-39.84	10.68	-29.25
Panel 8	sub1	-9.72	9.72	-33.75
	sub2	-29.17	29.17	-29.25
Panel 9	sub1	-3.56	13.28	-33.75
	sub2	-10.68	39.84	-29.25
Panel 10	sub1	3.56	13.28	-33.75
	sub2	10.68	39.84	-29.25
Panel 11	sub1	9.72	9.72	-33.75
	sub2	29.17	29.17	-29.25
Panel 12	sub1	13.28	3.56	-33.75
	sub2	39.84	10.68	-29.25

Appendix C

Supplementary Figure of Results

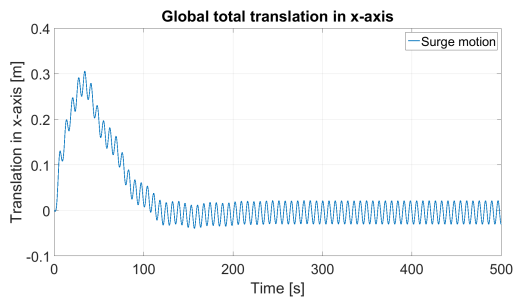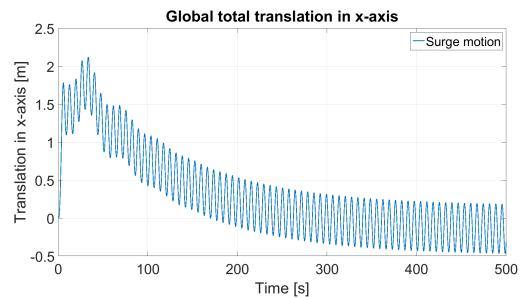Surge motion amplitude under the 12 wave states are appended below.
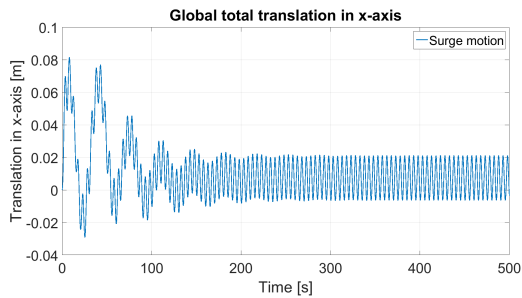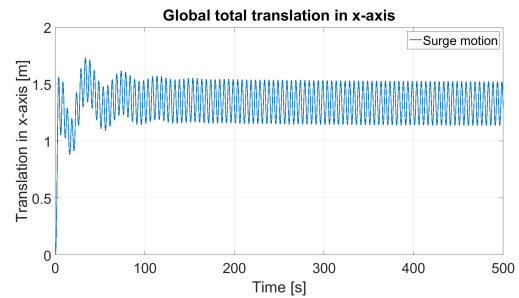
(a) $H_s = 1$m
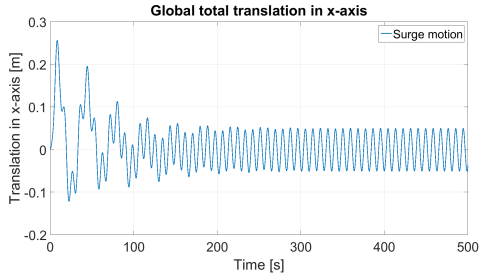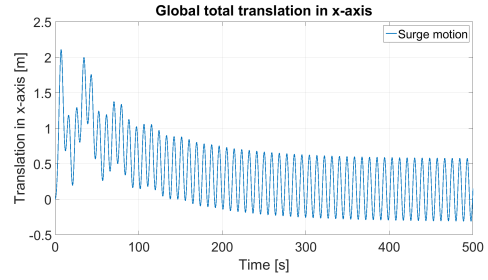
(b) $H_s = 5$m

Figure C.1: Surge motion when $T_P = 5$s

(a) $H_s = 1$m

(b) $H_s = 5$m

Figure C.2: Surge motion when $T_P = 7$s

(a) $H_s = 1$m

(b) $H_s = 5$m
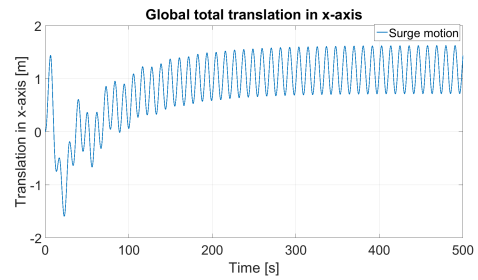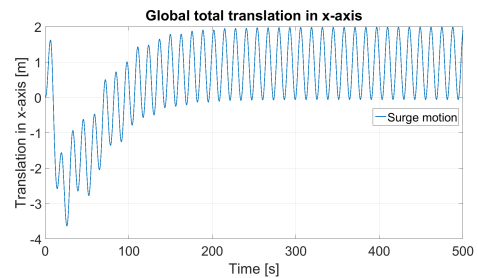
Figure C.3: Surge motion when $T_P = 9$s
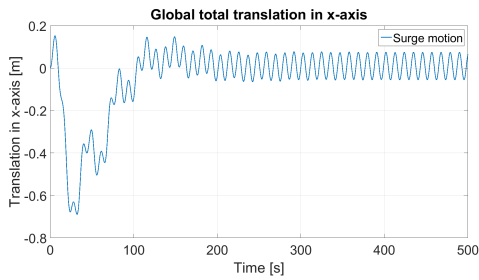
(a) $H_s = 1$m

(b) $H_s = 5$m

Figure C.4: Surge motion when $T_P = 11$s
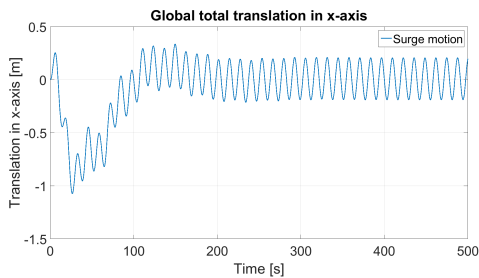
(a) $H_s = 1$m

(b) $H_s = 5$m

Figure C.5: Surge motion when $T_P = 13$s
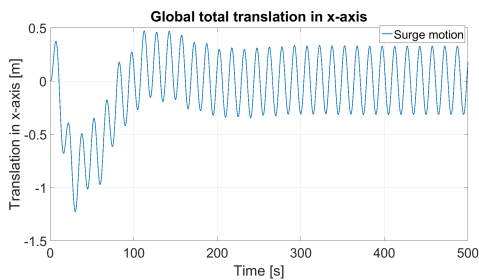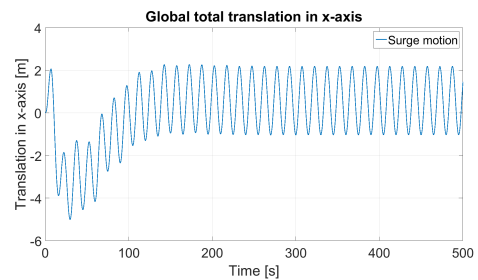
(a) $H_s = 1$m

(b) $H_s = 5$m

Figure C.6: Surge motion when $T_P = 15$s

Heave motion amplitude under the 12 wave states are appended below.

(a) $H_s = 1$m

(b) $H_s = 5$m

Figure C.7: Heave motion when $T_P = 5$s

(a) $H_s = 1$m

(b) $H_s = 5$m

Figure C.8: Heave motion when $T_P = 7$s

(a) $H_s = 1$m

(b) $H_s = 5$m

Figure C.9: Heave motion when $T_P = 9$s

(a) $H_s = 1$m

(b) $H_s = 5$m

Figure C.10: Heave motion when $T_P = 11$s

(a) $H_s = 1$m

(b) $H_s = 5$m

Figure C.11: Heave motion when $T_P = 13$s
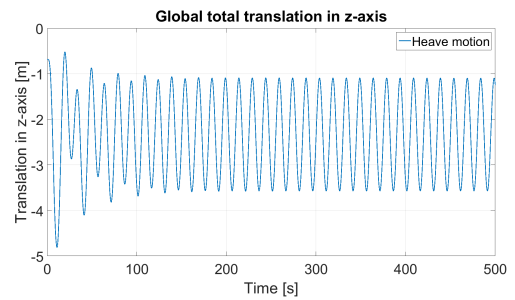
(a) $H_s = 1$m

(b) $H_s = 5$m

Figure C.12: Heave motion when $T_P = 15$s

Pitch motion amplitude under the 12 wave states are appended below.
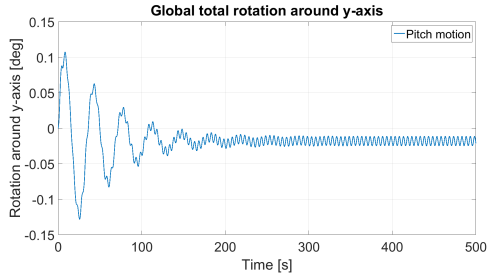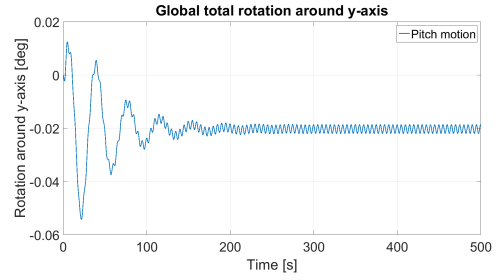
(a) $H_s = 1$m

(b) $H_s = 5$m

Figure C.13: Pitch motion when $T_P = 5$s
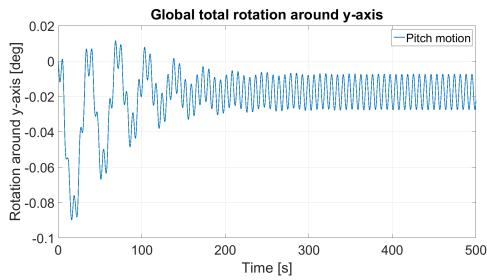
(a) $H_s = 1$m
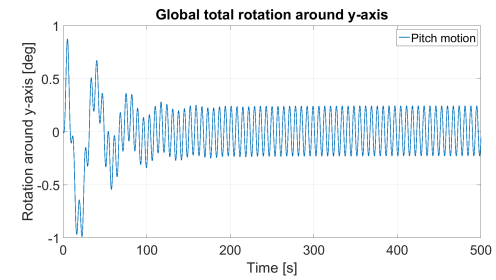
(b) $H_s = 5$m

Figure C.14: Pitch motion when $T_P = 7$s
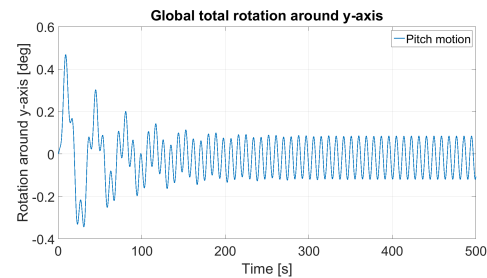
(a) $H_s = 1$m
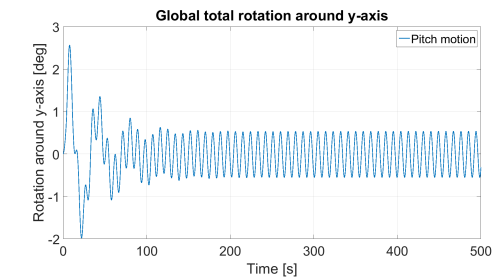
(b) $H_s = 5$m

Figure C.15: Pitch motion when $T_P = 9$s
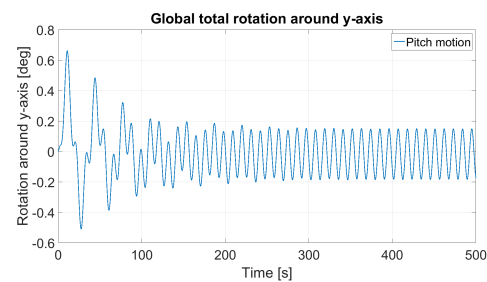
(a) $H_s = 1$m
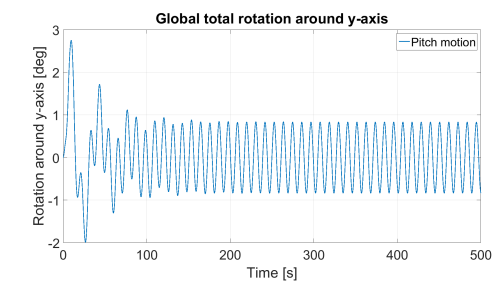
(b) $H_s = 5$m

Figure C.16: Pitch motion when $T_P = 11$s
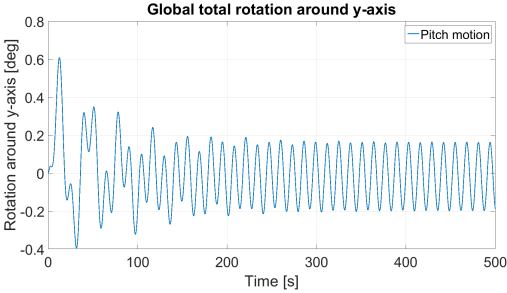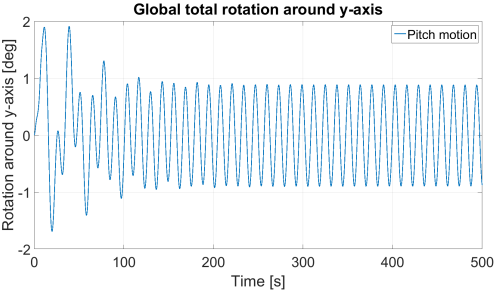
(a) $H_s = 1\text{m}$

(b) $H_s = 5\text{m}$

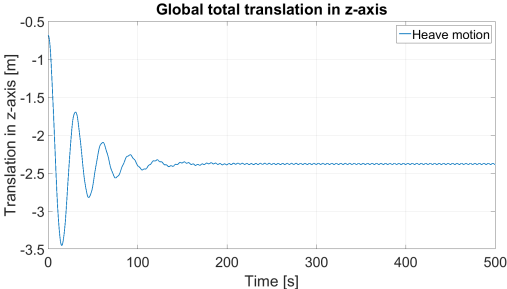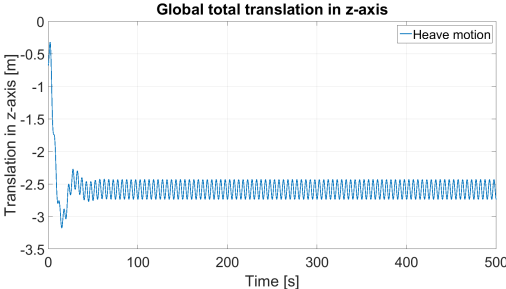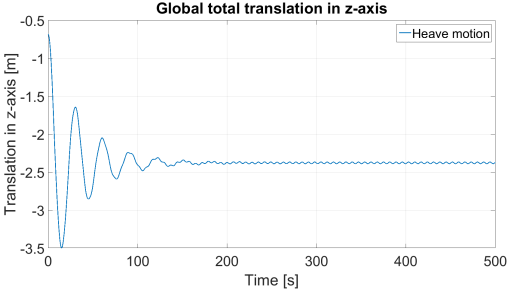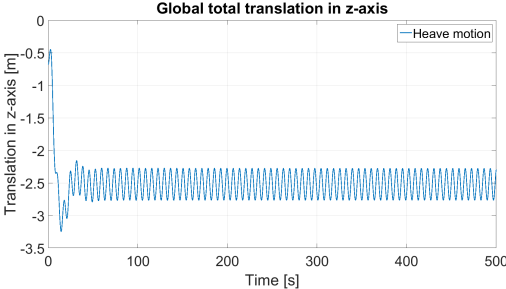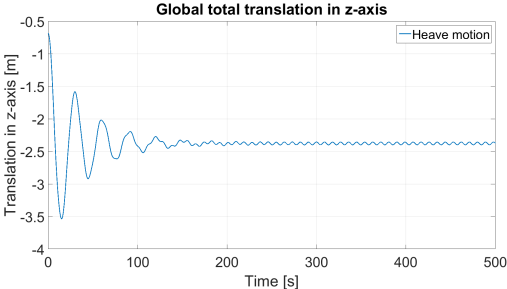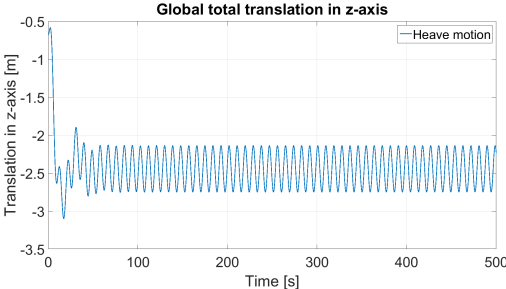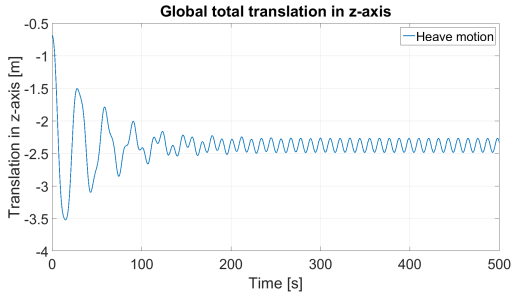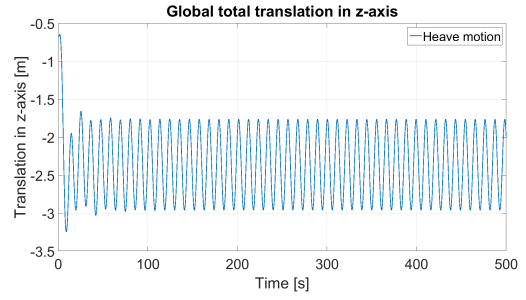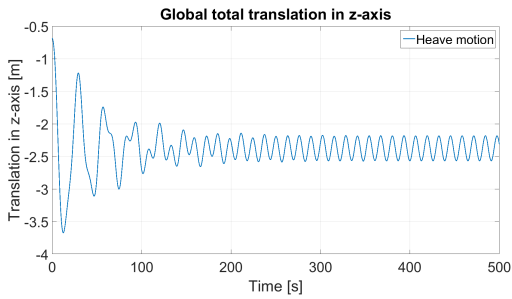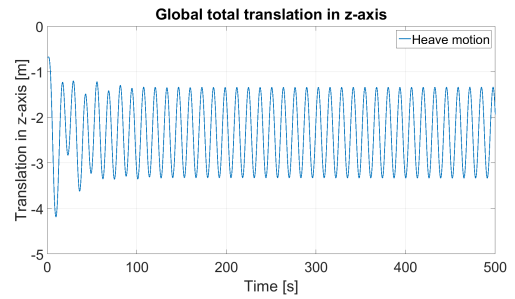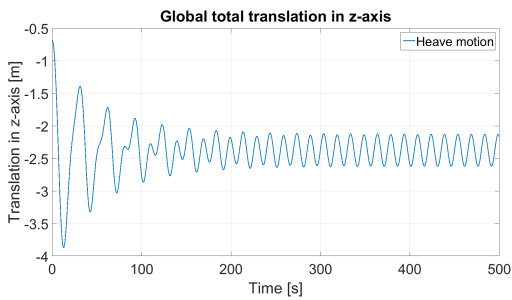Figure C.17: Pitch motion when $T_P = 13\text{s}$
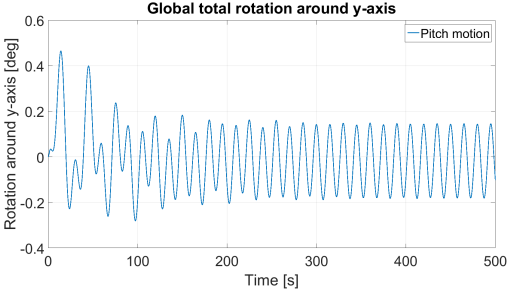
(a) $H_s = 1\text{m}$
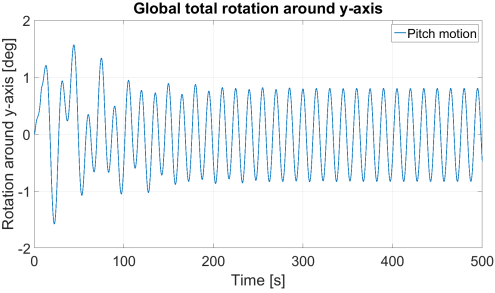
(b) $H_s = 5\text{m}$

Figure C.18: Pitch motion when $T_P = 15\text{s}$

Appendix D

Codes and Scripts

D.1 Matlab Code for Net Panel Calculation

The following code shows the step for sub-net panel calculation

Matlab code for sub-net panel calculations

```matlab
1   clear all , close all , clc
2   %% input information
3   L    = 55;                    % radial bottom beam length
4   a1   = 2*sin(15/180*pi)*L;    % width of total net panel
5   b1   = -30;                   % height of total net panel
6   z1   = linspace(0,b1,7);
7   alpha        = 30*linspace(0,-11,12);
8   Cx           = cosd(alpha)*55;
9   Cy           = sind(alpha)*55;
10  SubNetPanelS= zeros(3,9,12);
11  sn           = 0.161;
12  Aside        = abs(a1*b1);
13  AsubnetS     = Aside/9;
14  %% side sub net panel center coord
15  for i=1:12
16      if i==12
17      x = linspace(Cx(i),Cx(1),7);
18      y = linspace(Cy(i),Cy(1),7);
19      else
20      x = linspace(Cx(i),Cx(i+1),7);
21      y = linspace(Cy(i),Cy(i+1),7);
22      end
23      SubNetPanelS(1,:,i) = [x([2,4,6]),x([2,4,6]),x([2,4,6])];
24      SubNetPanelS(2,:,i) = [y([2,4,6]),y([2,4,6]),y([2,4,6])];
25      SubNetPanelS(3,:,i) = z1([2,2,2,4,4,4,6,6,6]);
26  end
27  %% bottom sub net panel center coord
28  L2       = linspace(0,55,5);
29  z2       = linspace(-27,-36,5);
30  SubNetPanelB = zeros(3,2,12);
31  SubNetPanelB (1,1,:) = L2(2)* cosd(alpha-15);
```

```matlab
32  SubNetPanelB (1,2,:) = L2(4)* cosd(alpha-15);
33  SubNetPanelB (2,1,:) = L2(2)* sind(alpha-15);
34  SubNetPanelB (2,2,:) = L2(4)* sind(alpha-15);
35  SubNetPanelB (3,1,:) = z2(4);
36  SubNetPanelB (3,2,:) = z2(2);
37  Abot      = 55*sind(15)*55*cosd(15)/cos(atan(7/51));
38  %% normal vector of net panel in local coordinates
39  for i=1:12
40      Ns(i,1) = cosd(alpha(i)-15);
41      Ns(i,2) = sind(alpha(i)-15);
42      Ns(i,3) = 0;
43      if Ns(i,1)<0
44          Ns(i,:)=-Ns(i,:);
45      end
46  end
47  for i=1:12
48      if i == 12
49          A = [cosd(alpha(i))*55,sind(alpha(i))*55,-27];
50          B = [cosd(alpha(1))*55,sind(alpha(1))*55,-27];
51      else
52          A = [cosd(alpha(i))*55,sind(alpha(i))*55,-27];
53          B = [cosd(alpha(i+1))*55,sind(alpha(i+1))*55,-27];
54      end
55      C = [0,0,-36];
56      a = A-C;
57      b = B-C;
58      c = cross(b,a);
59      L = sqrt(c(1)^2+c(2)^2+c(3)^2);
60      NB(i,:) = -c'/L;
61      if NB(i,1)<0
62          NB(i,:) = -NB(i,:);
63      end
64  end
65  A = [Aside,Abot];
66  save ('PNVLS.dat','Ns','-ASCII');
67  save ('PNVLB.dat','NB','-ASCII');
68  save ('A.dat','A','-ASCII');
69  save ('SNPB.dat','SubNetPanelB','-ASCII');
70  save ('SNPS.dat','SubNetPanelS','-ASCII');
71  fid = fopen('SNPS.dat', 'r+');
72  fprintf(fid, '%f\n',SubNetPanelS);
73  fclose(fid);
74  fid = fopen('SNPB.dat', 'r+');
75  fprintf(fid, '%f\n',SubNetPanelB);
76  fclose(fid);
```

D.2 Fortran Code for External Force Calculation

Below is the external file for net force calculation under wave state $T_p = 11$s and $H_s = 5$m.

Example of Fortran code of external file

```fortran
1   SUBROUTINE GFEXFO(IWA,RWA,DWA,IPDMS,&
2             IINFO,RINFO,NPCUR,CURCOR,CURVEL,&
3             KXFO,RXFO,RHXFO,&
4             IXFO,IEXTF,ICOORD,NINT,NREA,NSTO,NSTR,&
5             CHEXT,STATE,GAMMA,VELLOT,STOR,IERR)
6       !DEC$ ATTRIBUTES DLLEXPORT, ALIAS :"gfexfo_"::GFEXFO
7       !DEC$ ATTRIBUTES STDCALL::    GFEXFO
8       !DEC$ ATTRIBUTES REFERENCE:: IWA,RWA,DWA,IPDMS
9       !DEC$ ATTRIBUTES REFERENCE:: IINFO,RINFO,NPCUR,CURCOR,CURVEL
```

```fortran
10        !DEC$ ATTRIBUTES REFERENCE:: KXFO,RXFO,RHXFO
11        !DEC$ ATTRIBUTES REFERENCE:: IXFO, IEXTF ,ICOORD,NINT,NREA,NSTO,NSTR
12        !DEC$ ATTRIBUTES REFERENCE:: CHEXT,STATE,GAMMA,VELLOT,STOR,IERR
13        IMPLICIT NONE
14        !%%%%%%%%%%%%%%%%%%%%%%%%%%%%%%
15        ! - Internal variables
16        !%%%%%%%%%%%%%%%%%%%%%%%%%%%%%%
17        INTEGER IERR          !internal error flag code,  -- <0 error detected; =0 no error; >0 warning
18        INTEGER LAB           !?
19        !%%%%%%%%%%%%%%%%%%%%%%%%%%%%%%
20        ! - External variables
21        !%%%%%%%%%%%%%%%%%%%%%%%%%%%%%%
22        INTEGER, INTENT(IN):: IWA(*),IPDMS(*),ICOORD          ! internal work *array*;
23                                                              ! pointers to work *array*;
24                                                              ! flag for type of coordinate system for external force: 0 global coord; 1 ...
                                                                  local coord
25        INTEGER, INTENT(IN):: IINFO(*),NPCUR,KXFO(*),IXFO,NINT,NREA,NSTO,NSTR
26        ! integer information *array(12)*
27        ! Number of points where current velocities are given
28        ! integer external force parameter *array*
29        ! external force number
30        ! number of integer parameters
31        ! number of real parameters
32        ! number of parameters for intermediate storage
33        ! number of input strings
34        REAL, INTENT(IN)   :: RWA(*),RINFO(*),CURCOR(3,*),CURVEL(3,*)
35        ! real work *array*
36        ! real information *array(6)*
37        ! coordinates *array* of NPCUR points
38        ! current velocity *array* for NPCUR points
39        REAL                :: RXFO(*),RHXFO(NSTO)   ! real external force parameters
40                                                     ! array of intermediate storage
41        DOUBLE PRECISION, INTENT(IN):: STATE(12,*),GAMMA(9,*),VELLOT(6,*)
42        ! state variables (positions and velocities),
43        ! coordinate transformation matrix
44        ! local total velocity
45        REAL, INTENT(OUT)  :: STOR(*)   ! array of storage on file, 9 variables
46        DOUBLE PRECISION DWA(*)         ! double precision work array
47        CHARACTER*120 CHEXT(MAX(NSTR,1))! NSTR character strings as input
48        CHARACTER(*), PARAMETER :: fileplace = 'H:\thesis\'
49        INTEGER ISTO, ISTEP, IBODY, NBDY, NDIM, NSTEP, ITER, IEXTRA, NEXTRA,IEXTF,MODUL
50        REAL   TIME,DT,GRAV,RHOW,RHOA
51        ! %%%%% variable for structure, position, velocity %%%%%
52        DOUBLE PRECISION XG,YG,ZG,VX,VY,VZ
53        ! %%%% variable for environment, current,wave velocity %%%%
54        DOUBLE PRECISION VCX,VCY,VCZ,VWX,VWZ,ZETA0,T,OMEGA,K,UWAVESUBS(9,12),WWAVESUBS(9,12),UWAVESUBB(2,12),WWAVESUBB(2,12)
55        ! %%%%%%%%%%%%%%%%% variable for net panel %%%%%%%%%%%%%%%%
56        DOUBLE PRECISION SPNVL(3,12),SPNVG(3,12),BPNVL(3,12),BPNVG(3,12),RMV(3),SN,A(2),AS1,AB1(2),&
57                 SNPBL(3,2,12),SNPSL(3,9,12),SNPBG(3,2,12),SNPSG(3,9,12),X,Y,Z
58        INTEGER AS,AB
59        ! %%%%%%%%% variable for relative motion and force %%%%%%%%
60        DOUBLE PRECISION COSTHETAS(9,12),CDS(9,12),COSTHETAB(2,12),CDB(2,12),&
61                 FDS(9,12),FDB(2,12),FDSX(9,12),FDBX(2,12),FDSY(9,12),FDBY(2,12),FDSZ(9,12),FDBZ(2,12),MS(3,9,12),MB(3,2,12)
62        INTEGER I,J
63        DOUBLE PRECISION TI, PI
64        PI = 3.1415926
65        !%%%%%%%%%%%%%%%%%%%%%%%%%%%%%%%%%%%
66        ! - elements in IINFO
67        !%%%%%%%%%%%%%%%%%%%%%%%%%%%%%%%%%%%
68        MODUL  = IINFO(2);   ! Module
69        IBODY  = IINFO(3);   ! body number
70        ISTEP  = IINFO(6);   ! step number
71        NSTEP  = IINFO(7);   ! number of steps
72        IEXTRA = IINFO(8);   ! substep number
73        NEXTRA = IINFO(9);   ! number of substeps
74        ITER   = IINFO(12);  ! iteration no. in current step
75        !%%%%%%%%%%%%%%%%%%%%%%%%%%%%%%%%%%%
76        ! - elements in RINFO
77        !%%%%%%%%%%%%%%%%%%%%%%%%%%%%%%%%%%%
78        TIME = RINFO(1); ! actual total time
79        DT   = RINFO(2); ! time step length
80        GRAV = RINFO(3); !acceleration of gravity
81        RHOW = RINFO(4);   ! density of water
82        RHOA = RINFO(5); ! desity of air
83        TI   = TIME;
84        !%%%%%%%%%%%%%%%%%%%%%%%%%%%%%%%%%%%
85        ! - motion information
86        !%%%%%%%%%%%%%%%%%%%%%%%%%%%%%%%%%%%
87        XG = STATE(1,IBODY) ! global positions of COG of of the body
88        YG = STATE(2,IBODY)
89        ZG = STATE(3,IBODY)
90        VX = STATE(7,IBODY) ! global velocity of the body
91        VY = STATE(8,IBODY)
92        VZ = STATE(9,IBODY)
93        VCX = CURVEL(1,1)    ! current velocity
94        VCY = CURVEL(2,1)
95        VCZ = CURVEL(3,1)
96        !%%%%%%%%%%%%%%%%%%%%%%%%%%%%%%%%%%%
97        ! - data from matlab
98        !%%%%%%%%%%%%%%%%%%%%%%%%%%%%%%%%%%%
99        OPEN(101, FILE = fileplace//'PNVLS.dat')
100       Read(101,*) SPNVL ! PANEL NORMAL VECTOR
101       CLOSE(101)
102       OPEN(102, FILE = fileplace//'A.dat')
103       Read(102,*) A   ! AREA OF LARGE PANEL
104       CLOSE(102)
105       OPEN(103, FILE = fileplace//'SNPB.dat')
106       Read(103,*) SNPBL!SUB NET PANEL (ACTING) POINT BOTTOM
107       CLOSE(103)
108       OPEN(104, FILE = fileplace//'SNPS.dat')
109       Read(104,*) SNPSL !SUB NET PANEL (ACTING) POINT BOTTOM
110       CLOSE(104)
111       OPEN(105, FILE = fileplace//'PNVLB.dat')
112       Read(105,*) BPNVL ! PANEL NORMAL VECTOR
113       CLOSE(105)
114       AS = A(1)
115       AB = A(2)
116       AS1 = AS/9
117       AB1(1) = AB/4
118       AB1(2) = AB1(1)*3
119       SN = 0.161
120       !%%%%%%%%%%%%%%%%%%%%%%%%%%%%%%%%%%%
121       ! - wave generation
122       !%%%%%%%%%%%%%%%%%%%%%%%%%%%%%%%%%%%
123       !-----------------------------------------!
124       !---- transfer PNVL,SNPL to global ----- ! S/B_PNVG, SNP_B/S_G
125       !-----------------------------------------!
126       DO I=1,12
127           CALL TRANSLTG(GAMMA(1:9,IBODY),SPNVL(:,I),SPNVG(:,I))
128           CALL TRANSLTG(GAMMA(1:9,IBODY),BPNVL(:,I),BPNVG(:,I))
129               DO J = 1,9
```

```fortran
130              CALL COORDTRANSLTG(STATE(1:6,IBODY),SNPSL(:,J,I),SNPSG(:,J,I))
131          END DO
132          DO J = 1,2
133              CALL COORDTRANSLTG(STATE(1:6,IBODY),SNPBL(:,J,I),SNPBG(:,J,I))
134          END DO
135      END DO
136      !%%%%%%%%%%%%%%%%%%%%%%%%%%%%%%%%%
137      ! - wave generation
138      !%%%%%%%%%%%%%%%%%%%%%%%%%%%%%%%%%
139      !------------------------------------------!
140      !---- generate wave at each subpanel  ---- ! U/W_WAVESUB_S/B
141      !------------------------------------------!
142      T = 11
143      OMEGA = 2*PI/T
144      K = OMEGA**2/GRAV
145      ZETA0 = 2.5
146      DO I=1,12
147          DO J = 1,9
148              X = SNPSG(1,J,I);
149              Y = SNPSG(2,J,I);
150              Z = SNPSG(3,J,I);
151              UWAVESUBS(J,I) = OMEGA*ZETA0*EXP(K*Z)*SIN(OMEGA*TI-K*X);
152              WWAVESUBS(J,I) = OMEGA*ZETA0*EXP(K*Z)*COS(OMEGA*TI-K*X);
153          END DO
154          DO J = 1,2
155              X = SNPBG(1,J,I);
156              Y = SNPBG(2,J,I);
157              Z = SNPBG(3,J,I);
158              UWAVESUBB(J,I) = OMEGA*ZETA0*EXP(K*Z)*SIN(OMEGA*TI-K*X);
159              WWAVESUBB(J,I) = OMEGA*ZETA0*EXP(K*Z)*COS(OMEGA*TI-K*X);
160          END DO
161      END DO
162      !----------------------------------------------!
163      !---------  wave force calculation  ---------- !
164      !----------------------------------------------!
165      DO I = 1,12
166          DO J = 1,9
167              VWX = UWAVESUBS(J,I)
168              VWZ = WWAVESUBS(J,I)
169      !----  find relative motion of subnet panel ----- !
170              RMV(1) = VWX+VCX-VX
171              RMV(2) = 0-VY
172              RMV(3) = VWZ+VCZ-VZ
173              COSTHETAS(J,I) = dot_product(RMV,SPNVG(:,I))/NORM2(RMV)/NORM2(SPNVG(:,I))
174      !----  find Cd of each net panel  ----- !
175              CDS(J,I) = 0.04+(-0.04+0.33*SN+6.54*SN**2-4.88*SN**3)*ABS(COSTHETAS(J,I))
176              FDS(J,I) = 0.5*RHOW*CDS(J,I)*NORM2(RMV)**2*AS1
177              FDSX(J,I)= FDS(J,I)*RMV(1)/NORM2(RMV);
178              FDSY(J,I)= FDS(J,I)*RMV(2)/NORM2(RMV);
179              FDSZ(J,I)= FDS(J,I)*RMV(3)/NORM2(RMV);
180              CALL CROSS_PRODUCT(SNPSG(:,J,I),[FDSX(J,I),FDSY(J,I),FDSZ(J,I)],MS(:,J,I))
181          END DO
182          DO J = 1,2
183              VWX = UWAVESUBB(J,I)
184              VWZ = WWAVESUBB(J,I)
185      !----  find relative motion of subnet panel ----- !
186              RMV(1) = VWX+VCX-VX
187              RMV(2) = 0-VY
188              RMV(3) = VWZ+VCZ-VZ
189              COSTHETAB(J,I) = dot_product(RMV,BPNVG(:,I))/NORM2(RMV)/NORM2(BPNVG(:,I))
190      !----  find Cd of each net panel  ----- !
191              CDB(J,I) = 0.04+(-0.04+0.33*SN+6.54*SN**2-4.88*SN**3)*ABS(COSTHETAB(J,I))
192              FDB(J,I) = 0.5*RHOW*CDB(J,I)*NORM2(RMV)**2*AB1(J)
193              FDBX(J,I)= FDB(J,I)*RMV(1)/NORM2(RMV);
194              FDBY(J,I)= FDB(J,I)*RMV(2)/NORM2(RMV);
195              FDBZ(J,I)= FDB(J,I)*RMV(3)/NORM2(RMV);
196              CALL CROSS_PRODUCT(SNPBG(:,J,I),[FDBX(J,I),FDBY(J,I),FDBZ(J,I)],MB(:,J,I))
197          END DO
198      END DO
199      STOR(1) = (SUM(FDSX)+SUM(FDBX))
200      STOR(2) = (SUM(FDSY)+SUM(FDBY))
201      STOR(3) = (SUM(FDSZ)+SUM(FDBZ))
202      STOR(4) = (SUM(MS(1,:,:))+SUM(MB(1,:,:)))
203      STOR(5) = (SUM(MS(2,:,:))+SUM(MB(2,:,:)))
204      STOR(6) = (SUM(MS(3,:,:))+SUM(MB(3,:,:)))
205      !STOR(1)=100
206  END SUBROUTINE GFEXFO
207  !----------------------------------------------------------------------!
208  !------SUBROUTINE 01: coordinate transformation from local to global------!
209  !----------------------------------------------------------------------!
210  SUBROUTINE TRANSLTG(TMATRIX,XL,XG)
211  DOUBLE PRECISION, INTENT(OUT)::XG(3)
212  !$$$$$$ REAL, INTENT(IN)::TMATRIX(9),XL(3)
213  DOUBLE PRECISION, INTENT(IN)::TMATRIX(9)
214  DOUBLE PRECISION, INTENT(IN)::XL(3)
215  XG(1) = TMATRIX(1)*XL(1)+TMATRIX(2)*XL(2)+TMATRIX(3)*XL(3)
216  XG(2) = TMATRIX(4)*XL(1)+TMATRIX(5)*XL(2)+TMATRIX(6)*XL(3)
217  XG(3) = TMATRIX(7)*XL(1)+TMATRIX(8)*XL(2)+TMATRIX(9)*XL(3)
218  END SUBROUTINE TRANSLTG
219  !----------------------------------------------------------!
220  !------ SUBROUTINE 02: cross product to calculate moment------!
221  !----------------------------------------------------------!
222  SUBROUTINE CROSS_PRODUCT(VECT1,VECT2,VECTOUT)
223  DOUBLE PRECISION, INTENT(OUT)::VECTOUT(3)
224  !$$$$$$ REAL, INTENT(IN)::TMATRIX(9),XL(3)
225  DOUBLE PRECISION, INTENT(IN)::VECT1(3)
226  DOUBLE PRECISION, INTENT(IN)::VECT2(3)
227  vectout(1) = vect1(2) * vect2(3) - vect1(3) * vect2(2)
228  vectout(2) = vect1(3) * vect2(1) - vect1(1) * vect2(3)
229  vectout(3) = vect1(1) * vect2(2) - vect1(2) * vect2(1)
230  END SUBROUTINE CROSS_PRODUCT
231  !----------------------------------------------------------------------!
232  !------ SUBROUTINE 03: COORDINATES TRANSFER FROM LOCAL TO GLOBAL------!
233  !----------------------------------------------------------------------!
234  SUBROUTINE COORDTRANSLTG(BODYCOORD,VECT1,VECT2)
235  DOUBLE PRECISION, INTENT(OUT)::VECT2(3)
236  !$$$$$$ REAL, INTENT(IN)::TMATRIX(9),XL(3)
237  DOUBLE PRECISION, INTENT(IN)::VECT1(3)
238  DOUBLE PRECISION, INTENT(IN)::BODYCOORD(6)
239  VECT2(1) = BODYCOORD(1)+VECT1(3)*BODYCOORD(5)-VECT1(2)*BODYCOORD(6);
240  VECT2(2) = BODYCOORD(2)-VECT1(3)*BODYCOORD(4)+VECT1(1)*BODYCOORD(6);
241  VECT2(3) = BODYCOORD(3)+VECT1(2)*BODYCOORD(4)-VECT1(1)*BODYCOORD(5);
242  END SUBROUTINE COORDTRANSLTG
```